Macromolecules
ARTICLE

Macromolecules **2010**, *43*, 2589–2604 **2589**
DOI: 10.1021/ma902304x

Effect of the Electrostatic Interactions on Stretching of Semiflexible and Biological Polyelectrolytes

Jan-Michael Y. Carrillo and Andrey V. Dobrynin*

Polymer Program, Institute of Materials Science and Department of Physics, University of Connecticut, Storrs, Connecticut 06269-3136

Received October 16, 2009; Revised Manuscript Received January 15, 2010

ABSTRACT: Using combination of the molecular dynamics simulations and theoretical calculations, we have demonstrated that the bending rigidity of biological polyelectrolytes (semiflexible charged polymers) is force dependent. The effective chain bending rigidity decreases with increasing the value of the applied force. At small and intermediate values of the applied forces a semiflexible polyelectrolyte chain behaves similar to a neutral chain with the effective bending rigidity equal to the sum of the bare chain bending rigidity and electrostatic bending rigidity which has a well-known Odijk−Skolnick−Fixman (OSF) form with a quadratic dependence on the Debye radius. However, at large values of the applied force when the magnitude of the external force exceeds an electrostatic force responsible for the local chain stretching the effective chain bending rigidity is controlled by the bare chain elastic properties. This dependence of the bending rigidity on the applied force is a result of the scale dependent effect of the electrostatic interactions on the chain bending properties that can be approximated by two characteristic length scales. One describes the chain's elasticity at the distances along the polymer backbone shorter than the Debye screening length while another controls the long-scale chain's orientational correlations. By applying an external force to a semiflexible polyelectrolyte chain one probes different chain's deformation modes. Simulation results and theoretical model demonstrate a good quantitative agreement.

1. Introduction

Force spectroscopy experiments on DNA, RNA, actin, and microtubules filaments allow one to access information about stresses and strains experienced by molecules during biological process such as molecular recognition between DNA and proteins, protein induced bending of DNA, cytoskeleton polymerization, and energy transduction during the ATP cycle in molecular motors.[1−24] The techniques include hydrodynamic drag,[25−30] optical and magnetic tweezers,[15,31−35] and atomic force microscopy (AFM).[10,36−40] These methods probe a force range between 0.1 and 150 pN. In this force interval one can study both entropic and energetic effects on chain's elasticity. The interpretation of the force-elongation experiments and obtained values of the chain's elastic constants is model dependent and heavily relies on the assumptions used for the data analysis.[2,23,41,42]

The situation becomes even more complicated for DNA molecules for which the long-range electrostatic interactions play an important role in controlling chain's elastic properties.[41−51] The force−extension data of the double stranded DNA were described by a worm-like chain model[2,3,52] with the effective value of the chain's bending constant which has contributions from both the intrinsic chain's bending rigidity due to the base stacking and the electrostatic induced bending rigidity due to intrachain electrostatic repulsion.[43,44] This model is based on the assumption of the existence of the single length scale controlling chain's bending properties. However, the electrostatic interactions have a more complex effect on the bending properties of the semiflexible polyelectrolytes.[42,45,46,53] It was shown[53] that it is not sufficient to use a single correlation length to describe a decay of the bond−bond orientational correlations of a semiflexible polyelectrolyte chain. There are two different characteristic length scales that control short-range and long-range orientational memory along the polymer backbone.[53] The short-range correlation length describes chain orientational memory at the distances along the polymer backbone shorter or on the order of the Debye screening length. The long-range correlation length is responsible for chain's orientational correlations at distances longer than the Debye screening length. The reason for such chain behavior is the scale dependent effect of the electrostatic interactions on the chain's elastic and bending properties.[42,45,46,53]

In this paper we will apply our multiscale model[53] to study the effect of the electrostatic interactions on deformation of semiflexible polyelectrolyte chains. The rest of the paper is organized as follows. Section 2 presents results of the molecular dynamics simulations of semiflexible polyelectrolyte chain and shows how the applied external force changes the bond−bond correlation properties. In section 3, we present a model of the polyelectrolyte chain under tension. To test some of the model assumptions in section 4, we apply this model to describe force-elongation data of neutral semiflexible chains and derive a new crossover expression for dependence of the chain deformation on the magnitude of the applied force. This expression gives a better agreement with the simulation results and the exact solution[54] than the Marko−Siggia expression.[42] In section 5 we extend our analysis to include the effect of the electrostatic interactions on the chain's elastic and bending properties. Our analysis shows that the existence of two different characteristic length scales results in two different crossover regimes in dependence of the chain's orientational correlation lengths on the applied force. In section 6, we use our model to extract the effective chain's bending constant from force-elongation data and demonstrate that it is a force dependent. Finally, section 7 summarizes our results.

*Corresponding author.

Published on Web 02/04/2010

2. Molecular Dynamics Simulations of Chain Stretching

We have performed molecular dynamics simulations[55,56] of stretching of semiflexible polyelectrolyte chains by a constant force f. The model used for these simulations was similar to the one used in our study of the persistence length of semiflexible polyelectrolytes.[53] A polyelectrolyte chain was modeled by a bead−spring chain consisting of $N_m = 200$ charged particles (monomers) with diameter σ. The connectivity of the monomers into a chain was maintained by the finite extension nonlinear elastic (FENE) potential,

$$U_{FENE}(r) = -0.5k_{spring}R_{\max}{}^2\ln\left(1-\frac{r^2}{R_{\max}{}^2}\right) \quad (1)$$

where k_{spring} is the spring constant set to be $k_{spring} = 30k_BT/\sigma^2$ and $k_{spring} = 100k_BT/\sigma^2$, the maximum bond length is $R_{\max} = 1.5\sigma$, k_B is the Boltzmann constant and T is the absolute temperature. (The large value of the spring constant was selected to minimize the effect of the bond stretching at large values of the applied forces). The repulsive part of the bond potential was modeled by the truncated shifted Lennard-Jones potential with the values of the Lennard-Jones interaction parameter $\varepsilon_{LJ} = 0.34$ k_BT for $k_{spring} = 30k_BT/\sigma^2$ and $\varepsilon_{LJ} = 1.0\,k_BT$ for stronger bonds with $k_{spring} = 100k_BT/\sigma^2$. The chain bending rigidity was introduced into the model through a bending potential controlling the mutual orientations between two neighboring along the polymer backbone unit bond vectors $\vec{n}_i$ and $\vec{n}_{i+1}$

$$U^{bend}_{i,i+1} = k_BT\,K(1-(\vec{n}_i\cdot\vec{n}_{i+1})) \quad (2)$$

In our simulations the value of the bending constant K was varied between 25 and 160. For this chain model a chain persistence length l_p is proportional to the bending constant, $l_p = bK$, where b is the bond length.

We used a screened Coulomb potential

$$U_{el}(r_{ij}) = k_BT\,\frac{A_{el}\sigma}{r_{ij}}\exp(-\kappa r_{ij}) \quad (3)$$

to describe the electrostatic interactions between charged monomers on the polymer backbone separated by a distance r_{ij}. In eq 3 the interaction parameter $A_{el} = e^2\alpha^2/\varepsilon k_BT\sigma = l_B\alpha^2/\sigma$ describes the strength of the electrostatic interactions in terms of the thermal energy k_BT between charged monomers carrying an effective charge αe in a medium with the dielectric permittivity ε and separated by a distance σ. $l_B = e^2/\varepsilon k_BT$ is the Bjerrum length. (Note that we use the Electrostatic System of units.[57] In the SI units[57] the Bjerrum length is equal to $l_B = e^2/(4\pi\varepsilon_0\varepsilon k_BT)$ where $\varepsilon_0 = 8.85\times10^{-12}C^2/m^2N$ is the dielectric permittivity of the vacuum.) In our simulations, we have assumed that a polyelectrolyte chain is uniformly charged and each monomer is carrying a fractional charge αe. The Debye screening length κ^{-1} in solution with salt concentration c_s is defined as $\kappa^2 = 8\pi l_Bc_s$.

The simulations were performed at a constant temperature, which was maintained by coupling the system to the Langevin thermostat.[56] The motion of monomers was described by the following equations,

$$m\frac{d\vec{v}_i(t)}{dt} = \vec{F}_i(t) - \xi\vec{v}_i(t) + \vec{F}^R_i(t) \quad (4)$$

where m is the bead mass, $\vec{v}_i(t)$ is the bead velocity, and $\vec{F}_i(t)$ denotes the net deterministic force acting on the ith bead. The stochastic force $\vec{F}^R_i(t)$ has a zero average value $\langle\vec{F}^R_i(t)\rangle$ and δ-functional correlations $\langle\vec{F}^R_i(t)\cdot\vec{F}^R_i(t')\rangle = 6k_BT\xi\delta(t-t')$. The friction coefficient ξ was set to $\xi = 0.143m/\tau_{LJ}$, where τ_{LJ} is the standard LJ-time $\tau_{LJ} = \sigma(m/k_BT)^{1/2}$. The velocity−Verlet algorithm with a time step $\Delta t = 0.01\tau_{LJ}$ was used for integration of the equations of motion eq 4. Simulations were performed using the following procedure: at the beginning of each simulation run, a polyelectrolyte chain in a random walk configuration was placed in the center of the simulation box. A pair of constant forces f was applied to the both ends of a chain pointing in opposite directions along z-axis (see Figure 1). The magnitude of the force was varied between 10^{-3} and 50 k_BT/σ. The system was pre-equilibrated for 2×10^7 MD steps. This was followed by a production run lasting 2×10^8 MD steps. Such long simulation runs were required in order to obtain a good averaging of the bond−bond correlation function at large separations along the polymer backbone. Note that relatively short chains in our simulations were selected to minimize the chain's swelling effects on the bond−bond orientational correlations. In parts a and b of Figure 2, we show the dependence of the mean-square average end-to-end distance of a chain on the value of the applied force

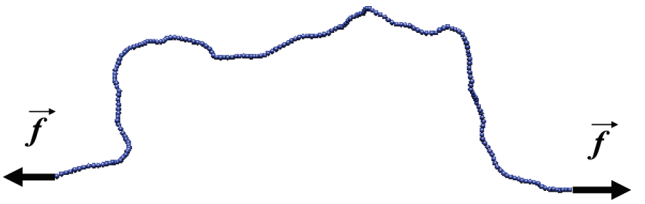

Figure 1. Polymer chain with applied forces.

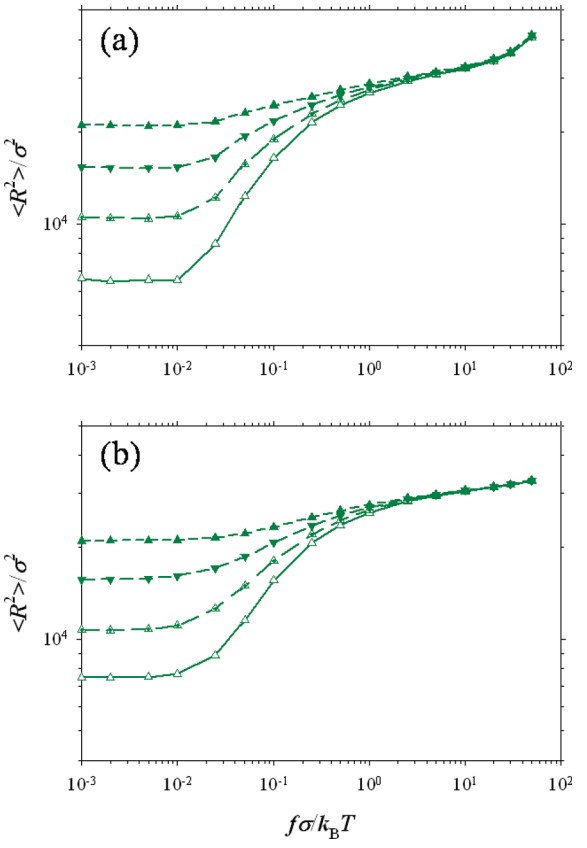

Figure 2. Dependence of the mean square average end-to-end distance $< R^2 >/\sigma^2$ on the magnitude of the applied force $f\sigma/k_BT$ for semiflexible polyelectrolyte chains with the degree of polymerization, $N_m = 200$, bending rigidity, $K = 25.0$, electrostatic coupling constant $A_{el} = 1.0$, bond potential parameters $k_{spring} = 30k_BT/\sigma^2$ (a), $k_{spring} = 100k_BT/\sigma^2$ (b) and for different values of the Debye screening length: $\kappa^{-1} = 5.0\sigma$ (half-filled triangles), $\kappa^{-1} = 10.0\sigma$ (inverted triangles) and $\kappa^{-1} = 20.0\sigma$ (filled triangles). Neutral chain results are shown by open triangles.

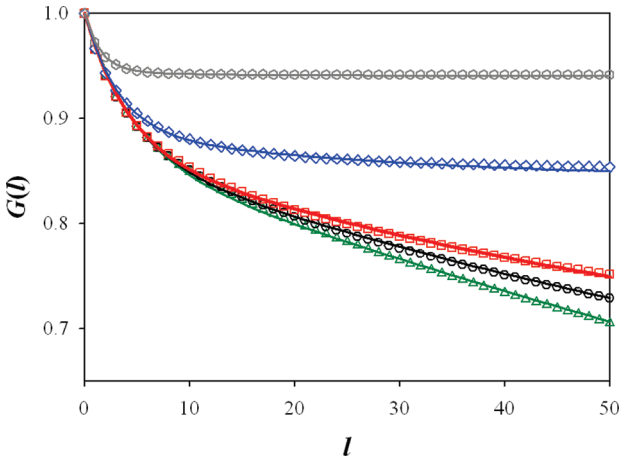

Figure 3. Bond-bond correlation functions of semiflexible polyelectrolyte chains with the degree of polymerization $N_m = 200$, the bond spring constant $k_{spring} = 100.0k_BT/\sigma^2$, the Lennard-Jones interaction parameter $\varepsilon_{LJ} = 1.0k_BT$, the bending constant $K = 25.0$, the electrostatic coupling constants $A_{el} = 1.0$, the Debye screening length $\kappa^{-1} = 20\sigma$ and different values of the applied force: $f = 0.001k_BT/\sigma$ (green open triangles), $f = 0.05k_BT/\sigma$ (black open circles), $f = 0.1k_BT/\sigma$ (red open squares), $f = 1.0k_BT/\sigma$ (blue open rhombs), $f = 10.0k_BT/\sigma$ (gray open hexagons). Solid lines are the best fit to eq 7.

for polyelectrolyte chains at different values of the Debye screening lengths and for a neutral chain. As one can see all plots demonstrate qualitatively similar behavior. At small values of the applied force, $f\sigma/k_BT < 10^{-2}$, the chain size saturates at the value corresponding to the unperturbed chain size. At the intermediate values of the applied force the chain elongates as the magnitude of the applied force increases. In the interval of the large applied forces, $f\sigma/k_BT > 3$, all lines converge indicating the crossover to the universal regime where chain's elastic properties become independent of the strength of the electrostatic interactions and are controlled by the bare chain's elasticity. Note that the upturn in the chain size dependence for $f\sigma/k_BT > 20$ seen in Figure 2a is due to the bond stretching. The average bond length for the system shown in Figure 2a is equal to 0.922 for $f\sigma/k_BT < 2.5$ and increases to 1.03 for $f\sigma/k_BT = 50$. There is no such upturn in the case of the larger values of the spring elastic constant (see Figure 2b) for which the bond length varies between 0.905 and 0.93 for the same force interval.More detailed information about the effect of the applied force on chain's properties can be obtained by analyzing the bond−bond correlation function.

$$G(l) = \frac{1}{N-l}\sum_{s=0}^{N-l-1}\langle(\vec{n}_s\cdot\vec{n}_{s+l})\rangle \qquad (5)$$

In Figure 3, we show evolution of this function with the force magnitude for a polyelectrolyte chain with the bending constant $K = 25$, the value of the Debye screening length $\kappa^{-1} = 20\sigma$ and electrostatic coupling constant $A_{el} = 1.0$. To minimize the end effects in obtaining the average values of the bond−bond correlation functions we have only considered 100 bonds in the middle of the chain during the averaging procedure. Our simulations show that this correlation function has two different functional forms. For small values of the applied force the bond−bond orientational correlations are well described by a sum of two exponential functions, while at the large values of the applied forces the correlation function can be fitted to the sum of exponential and a constant. The appearance of the constant term in the bond−bond correlation function in the large force limit is a result of the chain orientation along the direction of the applied force. Thus, the general form of the bond−bond correlation function that can describe both limits is

$$G(l) = \langle n_z\rangle^2 + \gamma\exp\left(-\frac{|l|}{\lambda_1}\right) + \beta\exp\left(-\frac{|l|}{\lambda_2}\right) \qquad (6)$$

where $\langle n_z\rangle$ is the average projection of the unit bond vector on the force direction. Note that the parameters γ and β are not independent, they are related by a normalization condition $G(0) = 1$, which gives $1 = \langle n_z\rangle^2 + \gamma + \beta$. Taking this into account, we can rewrite eq 6 as follows

$$G(l) = \langle n_z\rangle^2 + (1 - \langle n_z\rangle^2 - \beta)\exp\left(-\frac{|l|}{\lambda_1}\right) + \beta\exp\left(-\frac{|l|}{\lambda_2}\right) \qquad (7)$$

In the limit of zero applied force $f = 0$ and $\langle n_z\rangle = 0$, this equation reduces to the correlation function proposed in our previous publication[53] to describe correlation properties of semiflexible polyelectrolyte chain. Existence of the two different correlation length scales λ_1 and λ_2 in the chain's bond−bond correlation function is a result of the 2-fold effect of the electrostatic interactions on the chain bending and elastic properties. The characteristic length scale λ_1 in the case of zero force describes chain's bending properties at the length scales larger than the Debye screening length and has a well-known OSF-like quadratic dependence[43,44] on the Debye screening length κ^{-1}, $\lambda_1 \approx K + 0.25A_{el}\sigma/b(\kappa b)^2$, where b is the bond length. The second length scale λ_2 describes chain deformation at the length scales on the order of the Debye screening length and in the limit of the large Debye screening lengths has a form characteristic of a chain under tension, $\lambda_2 \approx (K/\tilde{f}_e)^{1/2}$, where the effective force is due to electrostatic interactions between charged monomers, $\tilde{f}_e \approx -A_{el}(\sigma/b)\ln(\kappa b)$. We have applied eq 7 to fit our simulation data shown in Figure 3 by using λ_1, λ_2, β, and $\langle n_z\rangle$ as adjustable parameters. The number of points used for this fitting procedure was optimized to minimize the difference between average values of the projection of the unit bond vector on the z-axis $\langle n_z\rangle$ obtained from simulations and one from the fitting procedure. Figure 4 shows dependence of the difference $1 - \langle n_z\rangle^2 - \beta$, describing the weight of the first exponential function in the total bond−bond correlation function, on the force amplitude. As one can see the value of the parameter β tends to $1 - \langle n_z\rangle^2$, making the weight of the first exponential function to approach zero (see Figure 4). This indicates that at the large force limit, $f\sigma/k_BT \gg 1$, the bond−bond correlation function can be fitted to a sum of a constant and an exponential function. In this limit the value of the parameter β approaches $1/(\tilde{f}K)^{1/2}$, $\lambda_2 \propto (K/\tilde{f})^{1/2}$ and the bond−bond correlation function reduces to

$$G(l) = 1 + \frac{1}{\sqrt{\tilde{f}K}}\left(\exp\left(-\sqrt{\frac{\tilde{f}}{K}}|l|\right) - 1\right) \qquad (8)$$

where we defined a reduced force $\tilde{f} = fb/k_BT$ and used the following relationship for the average value of the projection $\langle n_z\rangle$ and magnitude of the applied force f, $\langle n_z\rangle^2 = (1 - (\tilde{f}K)^{-1/2})$. Dependence of the chain's bond−bond correlation function only on the bare chain bending constant K further supports our observation that in the large force limit the properties of the polyelectrolyte chain are similar to those of a neutral chain.

In Figure 5, we plot variations of the characteristic length scales λ_1 (long-range characteristic length) and λ_2 (short-range characteristic length) with the magnitude of the applied force. These characteristic length scales λ_1 and λ_2 have two different crossover regimes. At small values of the applied force the value

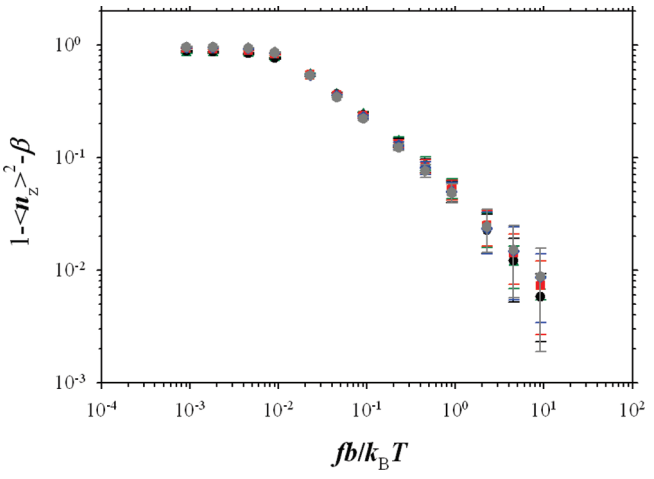

Figure 4. Dependence of the parameter $1-\langle n_z\rangle^2-\beta$ on the value of the applied force fb/k_BT for semiflexible polyelectrolyte chains with the degree of polymerization $N_m = 200$, bond spring constant $k_{spring} = 100.0k_BT/\sigma^2$, Lennard-Jones interaction parameter $\varepsilon_{LJ} = 1.0k_BT$, electrostatic coupling constant $A_{el} = 1.0$, for different values of the Debye screening length and bending constants: $\kappa^{-1} = 5\sigma$ and $K = 25.0$ (green half filled triangles); $\kappa^{-1} = 10\sigma$ and $K = 25.0$ (green inverted triangles); $\kappa^{-1} = 20\sigma$ and $K = 25.0$ (green filled triangles); $\kappa^{-1} = 20\sigma$ and $K = 40.0$ (black circles); $\kappa^{-1} = 20\sigma$ and $K = 80.0$ (red squares); $\kappa^{-1} = 20\sigma$ and $K = 120.0$ (blue rhombs); and $\kappa^{-1} = 20\sigma$ and $K = 160.0$ (gray hexagons).

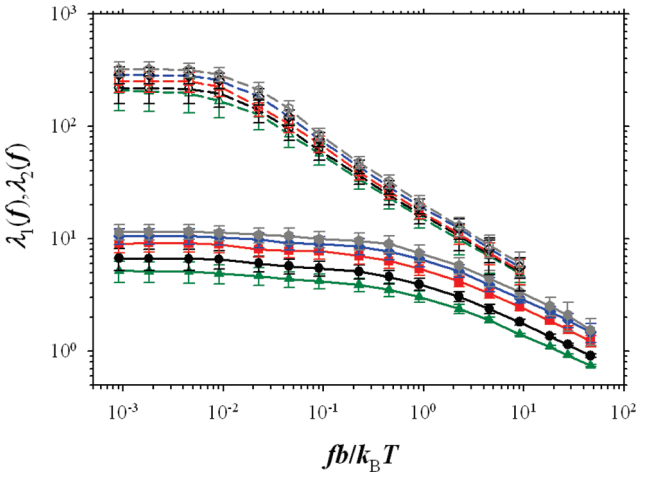

Figure 5. Dependence of the parameter $\lambda_1(f)$ (open symbols with dashed lines) and $\lambda_2(f)$ (filled symbols with solid lines) on the value of the reduced force fb/k_BT for semiflexible polyelectrolyte chains with the degree of polymerization $N_m = 200$, the bond spring constant $k_{spring} = 100.0k_BT/\sigma^2$, the Lennard-Jones interaction parameter $\varepsilon_{LJ} = 1.0\,k_BT$, the electrostatic coupling constant $A_{el} = 1.0$, the Debye screening length $\kappa^{-1} = 20\sigma$ and for different values of the bending constant: $K = 25.0$ (green triangles); $K = 40.0$ (black circles); $K = 80.0$ (red squares); $K = 120.0$ (blue rhombs); $K = 160.0$ (gray hexagons).

of the parameter λ_1 is constant. It starts to decrease with increasing the force magnitude at about $\tilde{f} \sim 10^{-2}$. In the larger force limit, $\tilde{f} > 10^{-2}$, the value of the parameter λ_1 is inversely proportional to the square-root of the applied force, $\lambda_1 \propto \tilde{f}^{-1/2}$ with a coefficient being proportional to $\lambda_1(0)^{1/2}$. This is exactly a scaling that one should expect if a polyelectrolyte chain is considered as a neutral chain with the effective bending constant $\lambda_1(0)$. The crossover to this regime is estimated to occur at $\tilde{f} \approx \lambda_1(0)^{-1}$. Unfortunately we have not been able to establish what happens with the parameter λ_1 in the limit of large forces, $\tilde{f} > 10$, because of the very small weight of the first exponential (see Figure 4) and uncertainty in the fitting procedure. In this force interval, the bond−bond correlation can be fitted to the function given by eq 8.

The second characteristic length scale λ_2 stays constant through the larger range of the applied forces up to $\tilde{f} \propto 1$. The crossover value of the force moves toward slightly larger force values with increasing the chain's bare bending constant K. Above the crossover value of the applied force this characteristic length scales decreases with increasing the value of the applied force as $\lambda_2 \approx (K/\tilde{f})^{1/2}$. Thus, in the large force limit both correlation lengths have similar force dependences.

In the next section, we present a theoretical model describing this peculiar polyelectrolyte chain behavior.

3. Theoretical Model of Stretching a Polyelectrolyte Chain

Consider a semiflexible polyelectrolyte chain with the number of bonds N, bond length b and fraction of charged monomers α, which ends are pulled by an external force with magnitude f pointing along z-axis. We can describe a chain conformation by a set of the unit vectors $\vec{n}_i$ pointing along the chain bonds. The potential energy of a semiflexible polyelectrolyte chain with the bending energy k_BTK in a given conformation includes the bending energy contribution, the electrostatic energy contribution and the contribution due to an external force

$$\frac{U_{PE}(\{\vec{n}_i\},\vec{f})}{k_BT} = \frac{K}{2}\sum_{i=0}^{N-2}(\vec{n}_i-\vec{n}_{i+1})^2 + \frac{l_B\alpha^2}{2}\sum_{i\neq j}^{N}\frac{\exp(-\kappa r_{ij})}{r_{ij}} - \sum_{i=0}^{N-1}\frac{b(\vec{f}\cdot\vec{n}_i)}{k_BT}, \quad (9)$$

where r_{ij} is the distance between monomers i and j on the polymer backbone. In evaluating contribution of the electrostatic interactions we will assume that a radius vector between monomers i and j along the polymer backbone is close to a straight line within the range of the exponential decay of the electrostatic potential. In this approximation we can approximate the distance between two monomers as follows

$$r_{ij} = b\sqrt{\left(\sum_{s=i}^{j-1}\vec{n}_s\right)^2} \approx bl_{ij}\left(1-\left(\frac{1}{4l_{ij}^2}\sum_{s,s'}(\vec{n}_s-\vec{n}_{s'})^2\right)\right) \quad (10)$$

where $l_{ij} = |j - i|$ is the number of bonds between ith and jth monomers along the polymer backbone. In obtaining eq 10 we used the identity:

$$(\vec{n}_s\cdot\vec{n}_m) = 1-(\vec{n}_s-\vec{n}_m)^2/2$$

Using eq 10, we can locally expand the electrostatic potential energy about a rod-like conformation and obtain the following correction to the electrostatic energy of a rod due to local chain bending

$$\frac{\Delta U_{elec}(\{\vec{n}_i\})}{k_BT} \approx \frac{u\alpha^2}{4}\sum_{i<j}^{N}\frac{\exp(-\kappa bl_{ij})}{l_{ij}^3}(1+\kappa bl_{ij})\left(\sum_{s,s'=i}^{j-1}(\vec{n}_s-\vec{n}_{s'})^2\right) \quad (11)$$

where u is the ratio of the Bjerrum length l_B to the bond size b. Note that the expansion eq 11 is correct as long as the chain's persistence length is larger than the Debye screening length κ^{-1}. Another comment worth making here is that the expansion eq 11 does not require for the whole chain to be close to a rod-like conformation and only assumes the local chain's orientational correlations. The partition function of a semiflexible

polyelectrolyte chain can be written as follows

$$Z(f) = \int d\{\vec{n}_i\} \exp\left(-\frac{U_{PE}(\{\vec{n}_i\},\vec{f})}{k_B T}\right) \tag{12}$$

where integration in eq 12 is performed over all orientations of the unit vectors $\vec{n}_i$.

In order to calculate averages with the partition function eq 12 it is useful to introduce the normal coordinates for a set of the bond vectors $\{\vec{n}_i\}$

$$\vec{n}_s = \sum_{k=-(N-1)}^{N-1} \vec{a}_k \exp\left(i\frac{\pi k s}{N}\right) \tag{13}$$

In the case when $\vec{a}_k = \vec{a}_{-k}$, eq 13 reduces to the cosine transform used in ref 53. In this representation, the chain's potential energy is a quadratic function of the mode amplitudes

$$\frac{U_{PE}(\{\vec{a}_k\},\vec{f})}{k_B T} = \frac{E_{rod}(b,\kappa)}{k_B T} + N \sum_{k=-(N-1)}^{N-1} \left(K\left(\frac{k\pi}{N}\right)^2 + V\left(\frac{k\pi}{N}\right)\right)\frac{(\vec{a}_k\cdot\vec{a}_{-k})}{2} - \frac{Nbf a_0^z}{k_B T} \tag{14}$$

where we defined

$$V(q) = 2u\alpha^2 \sum_{m=1}^{N}\left(1-\frac{m}{N}\right)\frac{\exp(-\kappa bm)}{m^3}(1+\kappa bm)\left(\sum_{s=1}^{m}(m-s)(1-\cos(qs))\right) \tag{15}$$

and the electrostatic energy of a charged rod is equal to

$$\frac{E_{rod}(b,\kappa)}{k_B T} = u\alpha^2 \sum_{l=2}^{N}(N-l)\frac{\exp(-\kappa bl)}{l} \tag{16}$$

The summation in eq 16 starts with $l = 2$ because in our simulations we have neglected the electrostatic interactions between neighboring along the polymer backbone charged monomers (1−2 electrostatic interactions). Also in writing eq 14 for the force term we kept only zero mode contribution by assuming that N is sufficiently large such that

$$\sum_{s=0}^{N-1} \exp(ik\pi s/N) \Rightarrow N\delta_{k,0}$$

(see Appendix A for details).

In normal mode representation, the bond−bond correlation function $G(l)$ describing the decay of the orientational memory along the polymer backbone

$$G(l) = \frac{1}{N-l}\sum_{s=0}^{N-l-1}\langle(\vec{n}_s\cdot\vec{n}_{s+l})\rangle \tag{17}$$

is equal to

$$G(l) = \sum_{k=-(N-1)}^{N-1}\langle(\vec{a}_k\cdot\vec{a}_{-k})\rangle \exp\left(i\frac{k\pi l}{N}\right) \tag{18}$$

It is important to point out that the normal modes are not independent. This is due to the constraint on the value of the bond−bond correlation function $G(l)$ at $l = 0$ which should be equal to unity

$$1 = \sum_{k=-(N-1)}^{N-1}\langle(\vec{a}_k\cdot\vec{a}_{-k})\rangle \tag{19}$$

In order to account for this constraint we will introduce a Lagrange multiplier μ, and modify the expression for the chain's potential energy as follows

$$\frac{U_{PE}(\{\vec{a}_k\},\vec{f},\mu)}{k_B T} = E_{rod}(b,\kappa) + N\sum_{k=-(N-1)}^{N-1}\left(K\left(\frac{k\pi}{N}\right)^2 + V\left(\frac{k\pi}{N}\right)+\mu\right)\frac{(\vec{a}_k\cdot\vec{a}_{-k})}{2} - \frac{N\mu}{2} - N\tilde{f}a_0^z \tag{20}$$

where we used the expression for a reduced force $\tilde{f} = fb/k_B T$. The complication in calculating averages with the chain's potential energy given by eq 20 arises because it requires knowledge of orientations of the vector $\vec{a}_0$. However, we can evaluate averages over mode amplitude $\vec{a}_0$ in two limiting cases of small and large values of the applied forces. In the small force limit we can consider the force term in the rhs of eq 20 as a perturbation. In this approximation the average value of the projection of the unit bond vector on the direction of the force is equal to

$$\langle n_z\rangle = \left\langle N^{-1}\sum_{s=0}^{N-1} n_s^z\right\rangle = \langle a_0^z\rangle \approx N\tilde{f}\langle(a_0^z)^2\rangle_0 = \frac{2\tilde{f}}{3\mu}, \quad \text{for } \tilde{f} \ll 1 \tag{21a}$$

where brackets $\langle\rangle$ and $\langle\rangle_0$ denote averages with the statistical weights corresponding to partition functions $Z(f)$ and $Z(0)$ respectively (see eq 12). In simplifying eq 21a we used the following relation:

$$\langle(a_0^z)^2\rangle_0 = \langle\vec{a}_0{}^2\rangle_0/3 = 2/(3\mu N)$$

In the case of the large force amplitudes we can assume that one of the components of the vector $\vec{a}_0$ points in the direction of the applied force while another is located in the xy-plane. Thus, the addition of the external constant force changes the average value of the amplitude of the component of the zero mode along z-axes to $\langle a_0^z\rangle = \tilde{f}/\mu$, resulting in the following expression for the value of

$$\langle n_z\rangle = \langle a_0^z\rangle = \frac{\tilde{f}}{\mu}, \quad \text{for } \tilde{f} \geq 1 \tag{21b}$$

The validity of eqs 21 for the average value of the projection is discussed in Appendix A. Note that the difference between eqs 21a and 21b is in the numerical coefficient. We can write a simple crossover expression which covers both limiting cases

$$\langle n_z\rangle = \frac{\tilde{f}}{\mu}\left(1-\frac{1}{3}\frac{\mu(0)}{(\mu(0)+\tilde{f})}\right) \tag{22}$$

where $\mu(0)$ is the value of the Lagrange multiplier at zero force. Taking this into account, we can rewrite the expression for the bond−bond correlation function

$$G(l) = \frac{2}{\pi}\int_0^\infty \frac{\cos(ql)\,dq}{Kq^2 + V(q) + \mu} + \langle n_z\rangle^2 \tag{23}$$

and the self-consistent equation for the Lagrange multiplier μ

$$1 = \frac{2}{\pi}\int_0^\infty \frac{dq}{Kq^2 + V(q) + \mu} + \langle n_z\rangle^2 \quad (24)$$

In writing eqs 23 and 24, we have introduced $q = k\pi/N$, substituted summation by integration and extended the upper integration limit to infinity. We also set $\vec{a}_k = \vec{a}_{-k}$ and took into account the fact that the normal mode representation (see eq 13) is a linear transformation such that the total number of independent components of the vectors $\{\vec{a}_k\}$ is equal to the total number of independent components of the vectors $\{\vec{n}_s\}$ that is equal to $2N$ because each vector $\vec{n}_s$ is a unit bond vector. A numerical solution of eq 24 gives functional dependence of the parameter μ on the magnitude of the external force f.

We can use the expression for the bond−bond correlation function $G(l)$ and calculate dependence of the chain size on the magnitude of the external force

$$\langle R^2(f)\rangle = b^2\sum_{i,j=0}^{N-1}\langle \vec{n}_i\cdot\vec{n}_j\rangle = b^2N + 2b^2\sum_{l=1}^{N}(N-l)G(l) \quad (25)$$

which can be reduced to

$$\frac{\langle R^2(f)\rangle}{b^2} = N + 2\sum_{l=1}^{N}(N-l)\frac{2}{\pi}\int_0^\infty \frac{\cos(ql)\,dq}{Kq^2 + V(q) + \mu} + \langle n_z\rangle^2 N(N-1) \quad (26)$$

We can further simplify eq 26 and perform summation over l. This leads to

$$\frac{\langle R^2(f)\rangle}{b^2} \approx \frac{8}{\pi}\int_0^\infty \frac{\sin^2\left(\frac{qN}{2}\right)dq}{q^2(Kq^2 + V(q) + \mu)} + \langle n_z\rangle^2 N^2 \quad (27)$$

In simplifying eq 27, we have used an expansion: $\sin q \approx q$. Note that eqs 24 and 27 provide expression for the force−deformation curve and allow incorporation of the intrachain electrostatic interactions into a model in a self-consistent manner for the entire range of the applied force. In this respect our model is different from the Marko and Siggia approach[42] to deformation of a semiflexible polyelectrolyte chain which is only correct in the limit of the large chain deformations. In the next section we will test our approximation by considering a deformation of neutral semiflexible chain and compare our results with the Marko−Siggia[42] and Bouchait et al[54] models.

4. Deformation of Neutral Semiflexible Chain

In the case of a neutral chain the value of the electrostatic potential $V(q) = 0$. In this case, the integral in the rhs of eq 24 can be analytically calculated resulting in

$$1 = \frac{1}{\sqrt{\mu K}} + \langle n_z\rangle^2 \quad (28)$$

with the value of the Lagrange multiplier $\mu(0) = K^{-1}$. Figure 6 shows dependence of the reduced value of the Lagrange multiplier μK on the reduced force fbK/k_BT. The data points for this plot were obtained from the average value of the projection of the unit bond vector on the direction of the applied force, $\langle n_z\rangle = \tilde{f}/\mu$, in the limit of the large force magnitudes and from mean square average value of fluctuation of this vector

$$\langle n_z^2\rangle - \langle n_z\rangle^2 = 1/(3\sqrt{\mu K})$$

in the limit of the small force magnitudes. There are two asymptotic regimes in dependence of the Lagrange multiplier

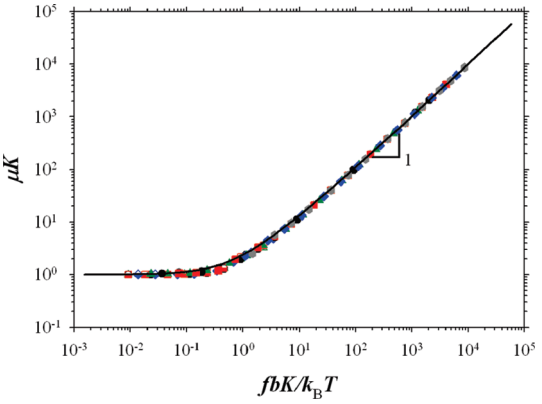

Figure 6. Dependence of the reduced value of the Lagrange multiplier μK on the reduced force fbK/k_BT for neutral semiflexible polymer chains with the degree of polymerization, $N_m = 200$, bond spring constant $k_{spring} = 30.0k_BT/\sigma^2$, Lennard-Jones interaction parameter $\varepsilon_{LJ} = 0.34\ k_BT$, and with different bending constants: $K = 1.0$ (green half-filled triangles), $K = 5.0$ (black half-filled circles), $K = 10.0$ (red half-filled squares), $K = 15.0$ (blue half-filled rhombs), $K = 25.0$ (green filled triangles), $K = 40.0$ (black filled circles), $K = 80.0$ (red filled squares), $K = 120.0$ (blue filled rhombs), and $K = 160.0$ (gray filled hexagons). Solid line corresponds to eq 28.

μ on the value of the applied force. In the case of weak chain deformations when the value of the reduced force is small, $\tilde{f}K \ll 1$, the value of the Lagrange multiplier is inversely proportional to the chain's bending constant and shows a quadratic dependence on the force magnitude

$$\mu \approx K^{-1}\left(1 + \frac{8}{9}(\tilde{f}K)^2\right) \quad (29)$$

In the opposite limit, $\tilde{f}K \gg 1$, the value of the Lagrange multiplier scales linearly with the magnitude of the applied force

$$\mu \approx \tilde{f} \quad (30)$$

The bond−bond correlation function is obtained by performing integration in eq 23 resulting in the following expression

$$G(l) = \frac{1}{\sqrt{\mu K}}\exp\left(-\sqrt{\frac{\mu}{K}}l\right) + \langle n_z\rangle^2 = 1 + \frac{1}{\sqrt{\mu K}}\left(\exp\left(-\sqrt{\frac{\mu}{K}}l\right) - 1\right) \quad (31)$$

Once again there are two different asymptotic regimes for the form of the bond−bond correlation function. At small values of the parameter $\tilde{f}K \ll 1$ the value of the Lagrange multiplier μ is equal to K^{-1}. In this limit the bond−bond correlation function decays exponentially with the number of bonds l along the polymer backbone. In the opposite limit, $\tilde{f}K \gg 1$, the form of the correlation function changes. At short distances along the polymer backbone, $l \le (K/\mu)^{1/2}$, the orientational correlations show initial linear decay, $G(l) \approx 1 - l/K$, with the characteristic length scale determined by the chain's bending constant K. However, at large separations along the polymer backbone the value of the correlation function saturates, $G(l) \approx 1 - 1/(\mu K)^{1/2}$, showing the appearance of the preferential chain's orientation determined by the direction of the applied external force. In Figure 7, we show the dependence of the bond−bond correlation function on the distance l along the polymer backbone obtained

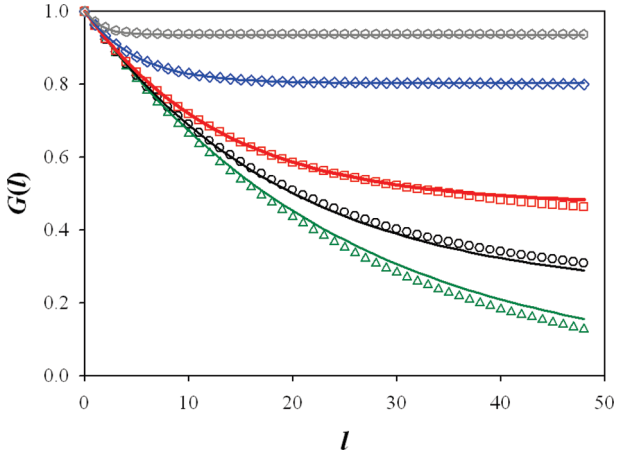

Figure 7. Bond-bond correlation functions of neutral semiflexible polymer chains with the degree of polymerization, $N_m = 200$, bending constant $K = 25.0$ and values of the applied force: $f = 0.001\ k_BT/\sigma$ (green open triangles), $f = 0.05\ k_BT/\sigma$ (black open circles), $f = 0.1\ k_BT/\sigma$ (red open squares), $f = 1.0\ k_BT/\sigma$ (blue open rhombs), and $f = 10.0\ k_BT/\sigma$ (gray open hexagons). Solid lines correspond to eq 31.

for different values of the applied forces. The lines on this plot correspond to analytically calculated correlation function given by eq 31. The agreement between simulation and analytical results is very good. It is important to point out that we used the value of the bond length b obtained from simulations to calculate the value of the Lagrange multiplier μ (see eq 28). The correction for the bond length becomes important for the large values of the applied forces, $f > 20\ k_BT/\sigma$, for which the bond length approaches 0.92σ.

Using an explicit form of the bond−bond correlation function we can calculate the chain size dependence on the magnitude of the external force.

$$\frac{\langle R^2(\mu(f))\rangle}{b^2} \approx \frac{g(\mu,K)}{\sqrt{\mu K}} + \left(1 - \frac{1}{\sqrt{\mu K}}\right) N^2 \tag{32}$$

where we introduced

$$g(\mu,K) = N\frac{1+\exp(-\sqrt{\mu/K})}{1-\exp(-\sqrt{\mu/K})} - 2\exp(-\sqrt{\mu/K})\frac{(1-\exp(-N\sqrt{\mu/K}))}{(1-\exp(-\sqrt{\mu/K}))^2} \tag{33}$$

For large values of the applied force, $\tilde{f}K \geq 1$, the chain size is a universal function of the reduced Lagrange multiplier μK or a reduced force $\tilde{f}K$ (see eq 28).

$$\frac{\langle R^2(f)\rangle}{b^2N^2} \approx 1 - \frac{1}{\sqrt{\mu K}} \approx 1 - \frac{1}{\sqrt{\tilde{f}K}} \tag{34}$$

The experimental data on chain deformation provide information about the force dependence of the average value of the projection of the chain's end-to-end distance on the direction of the applied force. This average value is equal to

$$\langle R_z\rangle = Nb\langle n_z\rangle = Nb\frac{\tilde{f}}{\mu}\begin{cases}\frac{2}{3}, & \text{for } \tilde{f}K \ll 1\\ 1, & \text{for } \tilde{f}K \gg 1\end{cases} \tag{35}$$

Using eq 28, we can transform eq 35 in a form which relates the chain's deformation ratio, $\langle n_z\rangle = \langle R_z\rangle/bN$, with the force

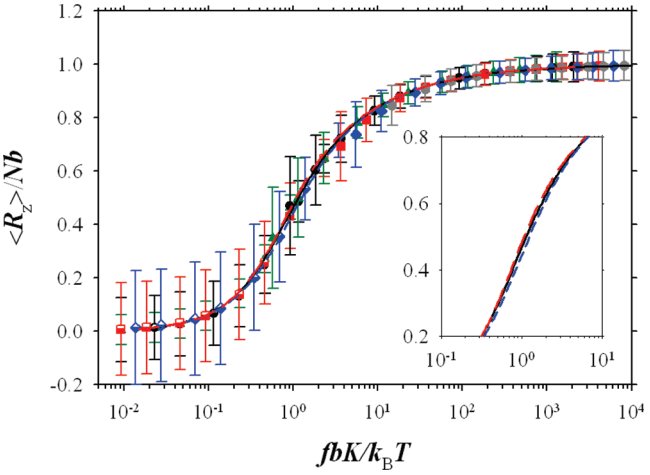

Figure 8. Dependence of the chain deformation ratio $\langle R_z\rangle/Nb$ on the magnitude of the reduced force fbK/k_BT for neutral semiflexible polymer chains with the degree of polymerization $N_m = 200$, bond spring constant $k_{spring} = 30.0\ k_BT/\sigma^2$, Lennard-Jones interaction parameter $\varepsilon_{LJ} = 0.34\ k_BT$ for different values of the bending constants: $K = 1.0$ (green half-filled triangles), $K = 5.0$ (black half-filled circles), $K = 10.0$ (red half-filled squares), $K = 15.0$ (blue half-filled rhombs), $K = 25.0$ (green filled triangles), $K = 40.0$ (black filled circles), $K = 80.0$ (red filled squares), $K = 120.0$ (blue filled rhombs), and $K = 160.0$ (gray filled hexagons). The solid line is given by eq 36, the red long-dashed line represents the exact solution by Bouchiat et al.,[54] and the blue short-dashed line corresponds to the Marko−Siggia expression.[42]

magnitude in both limits

$$\frac{fbK}{k_BT} = \frac{\langle n_z\rangle}{2} + \frac{\langle n_z\rangle}{(1-\langle n_z\rangle^2)^2} \tag{36}$$

In deriving eq 35 we solved eq 28 for the Lagrange multiplier μ as a function of $\langle n_z\rangle$ then substituted this solution into eq 35. In Figure 8 we apply eq 36 to collapse all our simulation data for neutral chains into one universal plot. The agreement between crossover expression and the simulation results is excellent. The error bars in the Figure 8 are proportional to $(g(\mu,K)/(3(\mu K)^{1/2}))^{1/2}$ and could be made smaller by considering longer chains. Note that our expression eq 36 is different from the crossover expression proposed by Marko and Siggia[42]

$$\frac{fbK}{k_BT} = \langle n_z\rangle + \frac{1}{4(1-\langle n_z\rangle)^2} - \frac{1}{4} \tag{37}$$

in the crossover regime. Their expression always underestimates chain deformation see Figure 8. The expression eq 36 is very close to the exact solution for the model of the worm like chain under tension obtained by Bouchiat et al.[54] The maximum difference for chain deformation between eq 36 and the exact solution is below 3% for $\langle n_z\rangle \sim 0.5$ while the difference between the exact solution and the Marko−Siggia expression[42] for the same deformation interval is close to 9%. Unfortunately, this difference between expressions is still smaller than the accuracy of the simulation data.

To the end of this section let us comment on how one can include bond deformation into our model. The details of calculations are given in Appendix B below we will only present the final result for the bond length dependence on the external force which was derived by approximating a bond potential energy by a parabolic function

$$b \approx b_0 + \frac{f\sigma^2}{K_{bond}k_BT} \tag{38}$$

where b_0 is the equilibrium bond length without applied force, and K_{bond}/σ^2 is the effective bond elastic constant in terms of the thermal energy k_BT. In the limit of the large deformations when the bond stretching effects become important eq 36 is transformed to

$$\langle R_z\rangle \approx Nb\left(1-\frac{1}{2}\left(\frac{fb}{k_BT}\right)^{-1/2}\right) \tag{39}$$

where the value of the bond length, b, is given by eq 38.

5. Effect of the Electrostatic Interactions on Chain Deformation

The presented above comparison of the simulation results with analytically calculated bond−bond correlation function and chain size shows that our model of deformation of semiflexible chain is in a good quantitative agreement with the simulation results. In this section, we will extend our analyses to describe deformation of the semiflexible polyelectrolyte chain.

In order to obtain an analytical expression for the force dependent bond−bond correlation function of a semiflexible polyelectrolyte chain and to understand the reason behind its form change with increasing the magnitude of the applied force we will evaluate integral in eq 24 by using a trial function approach developed in ref 53. It was shown in ref 53 that we can approximate function $V(q)$ by a trial function in the following form

$$V_{tr}(q) = \frac{Aq^2}{\delta^2+q^2} \tag{40}$$

Note that the form of the trial function $V_{tr}(q)$ can be established by considering the dependence of the electrostatic interaction potential $V(q)$ on the wavenumber q. In the limit $q\kappa b \ll 1$, this function is quadratic on q, $V(q) \propto q^2$, while in the opposite limit, $q\kappa b \gg 1$, it approaches a constant, $V(q) \propto -\ln(\kappa b)$. In the framework of the variational approach the parameters A and δ have to be found self-consistently from the normalization equation

$$1 = \frac{2}{\pi}\int_0^\infty \frac{dq}{\tilde{G}^{-1}(q)} - \frac{2}{\pi}\int_0^\infty \frac{(V(q)-V_{tr}(q))\,dq}{[\tilde{G}^{-1}(q)]^2} + \langle n_z\rangle^2 \tag{41}$$

where we introduced the bond−bond correlation function in q representation

$$\tilde{G}^{-1}(q) = Kq^2 + \frac{Aq^2}{\delta^2+q^2} + \mu \tag{42}$$

It is important to point out that the first integral in the rhs of eq 41 should be equal to 1-$\langle n_z\rangle^2$to satisfy the normalization condition for the norm of the unit bond vector because function $\tilde{G}(q)$ represents a fluctuation part of the bond−bond correlation function. Thus, eq 41 can be rewritten as two independent equations

$$1-\langle n_z\rangle^2 = \frac{2}{\pi}\int_0^\infty \frac{dq}{\tilde{G}^{-1}(q)},$$
$$\text{and}\quad \frac{2}{\pi}\int_0^\infty \frac{(V(q)-V_{tr}(q))\,dq}{[\tilde{G}^{-1}(q)]^2} = 0 \tag{43}$$

In order to evaluate the integrals in the eqs 43 it is useful to rewrite function $\tilde{G}(q)$ as

$$\tilde{G}(q) = \frac{1}{K(z_2^2-z_1^2)}\left[\frac{\delta^2-z_1^2}{q^2+z_1^2} + \frac{z_2^2-\delta^2}{q^2+z_2^2}\right] \tag{44}$$

where z_1 and z_2 are roots of the following equation

$$z^4 - (\delta^2+\mu/K+A/K)z^2 + \mu\delta^2/K = 0 \tag{45}$$

The bond−bond correlation function $G(l)$ corresponding to the function $\tilde{G}(q)$ has the following form

$$G(l) = \langle n_z\rangle^2 + (1-\langle n_z\rangle^2-\beta)\exp(-z_1|l|) + \beta\exp(-z_2|l|) \tag{46}$$

where the parameter β is defined as

$$\beta = \frac{z_2^2-\delta^2}{K(z_2^2-z_1^2)z_2} \tag{47}$$

This is exactly the correlation function observed in our simulations with roots $z_1 = 1/\lambda_1$ and $z_2 = 1/\lambda_2$ describing chain's correlation properties at the long and short length scales, respectively.

Substitution of the function $\tilde{G}(q)$, given by eq 44, into the first integral of eq 43 leads to

$$1 = \frac{\delta\sqrt{K}+\sqrt{\mu}}{K(z_1+z_2)\sqrt{\mu}} + \langle n_z\rangle^2 \tag{48}$$

The calculation details of the second integral and numerical solutions of the variational equations are given in Appendix C below we will present a scaling analysis of these solutions. It is useful to introduce a new variables x and y such that

$$z_1{}^2 = \frac{\mu}{x^2K},\quad z_2{}^2 = \frac{\mu}{y^2K},$$
$$\delta^2 = \frac{1}{xy}\sqrt{\frac{\mu}{K}},\quad \frac{A}{\delta^2} = K(x^2-1)(1-y^2) \tag{49}$$

and consider x, y, and μ as variational parameters. The analysis of eq C15 can be done analytically in the case $x \gg 1$ and $y \ll 1$. In this approximation the system of eqs C15 reduces to two simple equations

$$z_1I_1(z_1) - \frac{K}{2}(x^2-1) \approx 0 \tag{50a}$$

$$\frac{z_2^2I_1(z_2)}{(1-y^2)} - \frac{(\mu K)^{1/2}}{y} \approx 0 \tag{50b}$$

The function $I_1(z)$ has two different asymptotic regimes: $I_1(z) \approx K_{OSF}/(2z)$ for $z/(\kappa b) \ll 1$ and $I_1(z) \approx \tilde{f}_e/(2z^3)$ for $z/(\kappa b) \gg 1$ where we introduced the Odijk−Skolnick−Fixman electrostatic bending constant[43,44]

$$K_{OSF} = \frac{u\alpha^2}{4(\kappa b)^2} \tag{51}$$

and the effective electrostatic tension force

$$\tilde{f}_e = -u\alpha^2\ln(\kappa b) \tag{52}$$

The root z_2 describes chain's orientational correlations at the length scales smaller or on the order of the Debye screening length κ^{-1} such that $z_2/(\kappa b) \geq 1$. In this limit the expression eq 50b can be rewritten as

$$\frac{yK^{1/2}}{(1-y^2)\mu^{1/2}}\tilde{f}_e - \frac{(\mu K)^{1/2}}{y} \approx 0 \tag{53}$$

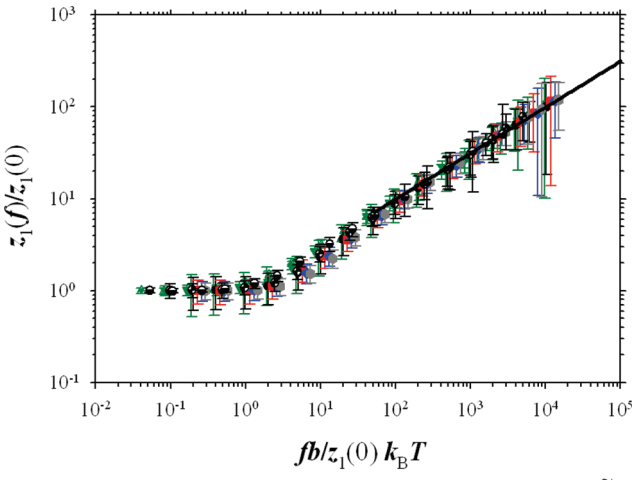

Figure 9. Dependence of the parameter $z_1(f)/z_1(0)$ on the reduced force $\tilde{f}/z_1(0)$ for semiflexible polyelectrolyte chains with the degree of polymerization $N_m = 200$, bond spring constant $k_{spring} = 100.0k_BT/\sigma^2$, Lennard-Jones interaction parameter $\varepsilon_{LJ} = 1.0k_BT$, electrostatic coupling constant $A_{el} = 1.0$ for different values of the Debye screening length and bending constants: $\kappa^{-1} = 5\sigma$ and $K = 25.0$ (green half filled triangles); $\kappa^{-1} = 10\sigma$ and $K = 25.0$ (green inverted triangles); $\kappa^{-1} = 20\sigma$ and $K = 25.0$ (green filled triangles); $\kappa^{-1} = 20\sigma$ and $K = 40.0$ (black circles); $\kappa^{-1} = 20\sigma$ and $K = 80.0$ (red squares); $\kappa^{-1} = 20\sigma$ and $K = 120.0$ (blue rhombs); and $\kappa^{-1} = 20\sigma$ and $K = 160.0$ (gray hexagons). The solid line has slope 0.5.

Solving this equation for the parameter y we obtain

$$z_2(\tilde{f}) \approx \frac{1}{y}\sqrt{\frac{\mu}{K}} \approx \sqrt{\frac{\tilde{f}_e+\mu}{K}} \tag{54}$$

The root z_1 describes the long-scale orientational correlations for which $z_1/(\kappa b) \le 1$. In this approximation the expression eq 50a reduces to

$$K_{OSF} - K(x^2-1) \approx 0 \tag{55}$$

Solving eq 55 for the parameter x we have

$$z_1(\tilde{f}) \approx \frac{1}{x}\sqrt{\frac{\mu}{K}} \approx \sqrt{\frac{\mu}{K^*}} \approx \begin{cases} 1/K^*, & \text{for } \tilde{f} \le K^{*-1} \\ \sqrt{\tilde{f}/K^*}, & \text{for } K^{*-1} \le \tilde{f} \le K^*(\kappa b)^2 \end{cases} \tag{56}$$

where we introduced

$$K^* = K + K_{OSF} \tag{57}$$

and approximated $\mu \approx 1/K^*$ for $\tilde{f}K^* \le 1$ and $\mu \approx \tilde{f}$ in the limit of large forces, $\tilde{f}K^* \ge 1$. It follows from eq 56 that the external applied force begins influence chain's correlation properties when the force amplitude $\tilde{f}$ exceeds $1/K^*$. In this interval of parameters the value of the Lagrange multiplier μ is equal to $\tilde{f}$ (see eq 48) and the smallest root z_1 of eq 45 is equal to $z_1 \approx (\tilde{f}/K^*)^{1/2}$. In this regime, at long-length scales, the chain behaves as a neutral chain with the effective bending rigidity K^* under the applied force $\tilde{f}$. However, the behavior of the chain at short-length scales is unchanged (see eq 54). This regime continues until the external force $\tilde{f}$ becomes on the order of the electrostatic tension force $\tilde{f}_e$. At larger values of the applied force, $\tilde{f} > \tilde{f}_e$, the second root z_2 shows $\tilde{f}^{1/2}$ dependence. Thus, at short-length scales the chain behavior is similar to that of a neutral chain with the effective bending constant K.

The value of the root $z_1 \approx (\tilde{f}/K^*)^{1/2}$ increases with increasing the force magnitude. It becomes on the order of the inverse Debye radius, $z_1 \approx \kappa b$, at $\tilde{f} \approx K^*(\kappa b)^2$. For larger values of the applied force $\tilde{f} > K^*(\kappa b)^2$ we have to use the second asymptotic expression for the function $I_1(z) \approx \tilde{f}_e/(2z^3)$. In this approximation, eq 50a transforms into

$$Kx^2\frac{\tilde{f}_e}{\mu} - K(x^2-1) \approx 0 \tag{58}$$

Solving this equation for the parameter x we obtain

$$z_1(\tilde{f}) \approx \frac{1}{x}\sqrt{\frac{\mu}{K}} \approx \sqrt{\frac{\tilde{f}-\tilde{f}_e}{K}}, \quad \text{for } \tilde{f} > K^*(\kappa b)^2 \tag{59}$$

Thus, asymptotically, the roots z_1 and z_2 (see eqs 54 and 59) should converge. It is also interesting to point out that in this force range the information about electrostatic interactions only enters through the electrostatic tension force $\tilde{f}_e$ responsible for the local chain deformation.

To illustrate relation of the different crossover regimes with the local chain tension and electrostatic renormalization of the chain's bending constant in Figures 9 and 10, we show normalized values of the roots z_1 and z_2 as functions of the reduced applied force. For the smallest root we plotted $z_1(\tilde{f})/z_1(0)$ as a function of $\tilde{f}/z_1(0)$, and for the largest root z_2 we used $z_2(\tilde{f})/z_2(0)$ for the y-axis and normalized the external force $\tilde{f}$ by $\tilde{f}_e = Kz_2^2(0)$. This choice of new reduced variables allowed us to collapse all our simulations data into universal plots confirming the existence of two different crossover regimes with $\tilde{f} \propto 1/K^*$ and $\tilde{f} \propto \tilde{f}_e$.

6. What Stretching Experiments Can Tell Us About the Chain's Bending Constant

The existence of the two different length scales controlling the chain's elastic and bending properties raises the question on how reliable the analysis of the experimental data on DNA stretching is when one assumes a single effective bending constant for the data interpretation.[2,3,52] To address this issue below, we perform analysis of the simulation data of a semiflexible polyelectrolyte chain and try to extract the effective chain's bending rigidity in order to demonstrate the effect of the different length scales on chain's effective bending constant. Comparing the expression eq 28 for a neutral chain with the expression eq 48 for a polyelectrolyte chain, we can introduce an effective chain bending constant K_{eff} such that

$$K_{eff} = \left(\frac{K(z_1+z_2)}{\delta\sqrt{K}+\sqrt{\mu}}\right)^2 = K\left(\frac{x+y}{1+xy}\right)^2 \tag{60}$$

where $x \approx (K^*/K)^{1/2}$ and $y \approx [\tilde{f}/(\tilde{f}_e+\tilde{f})]^{1/2}$ are solutions of the eqs 54 and 55. Using eq 60, we can rewrite eq 48 as follows

$$1 = \frac{1}{\sqrt{K_{eff}\mu}} + \langle n_z\rangle^2 \tag{61}$$

The effective bending rigidity K_{eff} can be viewed as a bending constant of a corresponding neutral chain. Using the neutral chain results (see eq 36) we can write the following parametric equation for a chain deformation ratio

$$\frac{fbK_{eff}}{k_BT} = \frac{\langle n_z\rangle}{2} + \frac{\langle n_z\rangle}{(1-\langle n_z\rangle^2)^2} \tag{62}$$

Note that we added an $\langle n_z\rangle/2$ term to cover the whole chain deformation range (see discussion in Section 4). We applied eq 62

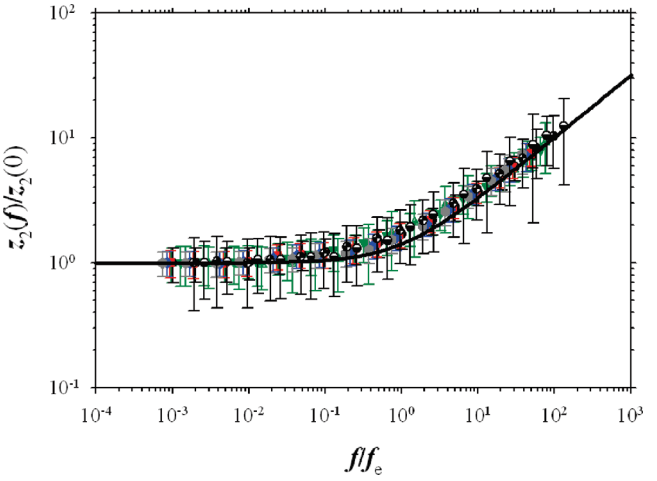

Figure 10. Dependence of the parameter $z_2(f)/z_2(0)$ on the reduced force $\tilde{f}/\tilde{f}_e$ where $\tilde{f}_e = z_2(0)^2K$ for semiflexible polyelectrolyte chains with the degree of polymerization $N_m = 200$, bond spring constant $k_{spring} = 100.0k_BT/\sigma^2$, Lennard-Jones interaction parameter $\varepsilon_{LJ} = 1.0k_BT$, electrostatic coupling constant $A_{el} = 1.0$ for different values of the Debye screening length and bending constants: $\kappa^{-1} = 5\sigma$ and $K = 25.0$ (green half filled triangles); $\kappa^{-1} = 10\sigma$ and $K = 25.0$ (green inverted triangles); $\kappa^{-1} = 20\sigma$ and $K = 25.0$ (green filled triangles); $\kappa^{-1} = 20\sigma$ and $K = 40.0$ (black circles); $\kappa^{-1} = 20\sigma$ and $K = 80.0$ (red squares); $\kappa^{-1} = 20\sigma$ and $K = 120.0$ (blue rhombs); and $\kappa^{-1} = 20\sigma$ and $K = 160.0$ (gray hexagons). The solid line is given by the equation $z_2(f)/z_2(0) = (1 + \tilde{f}/\tilde{f}_e)^{1/2}$.

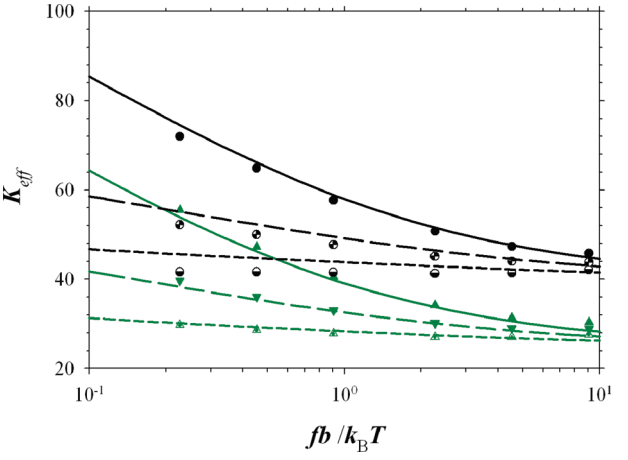

Figure 11. Dependence of the effective bending rigidity K_{eff} on the value of the applied force fb/k_BT for semiflexible polyelectrolyte chains with the degree of polymerization $N_m = 200$, the bond spring constant $k_{spring} = 100.0k_BT/\sigma^2$, the Lennard-Jones interaction parameter $\varepsilon_{LJ} = 1.0k_BT$, the electrostatic coupling constant $A_{el} = 1.0$ for different values of the Debye screening length and bending constants: $K = 25.0$ (green half filled triangles); $\kappa^{-1} = 10\sigma$ and $K = 25.0$ (green inverted triangles); $\kappa^{-1} = 20\sigma$ and $K = 25.0$ (green filled triangles); $\kappa^{-1} = 5\sigma$ and $K = 40.0$ (black half filled circles); $\kappa^{-1} = 10\sigma$ and $K = 40.0$ (black checkered circles); $\kappa^{-1} = 20\sigma$ and $K = 40.0$ (black filled circles). The lines correspond to numerically calculated values of the effective chain's bending constant K_{eff} (see text for details).

to extract K_{eff} from our simulation data for $\langle R_z(f)\rangle$. The results of this procedure are summarized in Figure 11. For this plot we used only data points for which chain's deformation exceeds 60% to minimize the error in obtaining value of the bending constant. As one can see from this plot the value of the effective bending constant decreases with increasing the value of the applied force. Also the lines corresponding to different values of the Debye screening length converge. This once again supports our observation that in the large force limit a polyelectrolyte chain behavior is similar to that of a neutral chain with the same value of the chain's bending constant. Note that the variations in the value of the effective bending constant are largest for the systems with the strongest electrostatic interactions corresponding to simulations with the larger values of the Debye screening lengths. Thus, the results in Figure 11 indicate that we can not use a force independent bending constant to fit the simulation data on chain deformation.

A qualitative understanding of the observed dependence of the effective chain's bending constant on the applied force could be obtained by analyzing eq 60. In the limit of small applied forces the parameter x is equal to $(K^*/K)^{1/2}$ (see eq 55) and the parameter y scales with the applied force as $[\tilde{f}/(\tilde{f}_e + \tilde{f})]^{1/2}$ (see eq 54). In the limit of $xy \ll 1$ and $x \gg 1$, the value of the effective bending constant can be approximated as $K_{eff} \approx K/x^2 \approx K^*$ (see eq 57). In this regime it is force independent and has a form used for interpretation of the DNA stretching data. However, it follows from eq 60 that this approximation is correct only if $xy \leq 1$ or

$$\tilde{f} \leq \tilde{f}_{K^*} \approx \tilde{f}_e \frac{K^* - K}{K} \approx \tilde{f}_e \frac{u\alpha^2}{4(\kappa b)^2 K} \tag{63}$$

where $\tilde{f}_{K^*}$ is the crossover value of the applied force at which $xy \approx 1$. The crossover value of the applied force depends on the bending constant K, the chain's degree of ionization α, and solution ionic strength I. We can estimate how this crossover value changes with the solution ionic strength for the DNA molecule. By approximating the charge distribution along the DNA backbone on the length scales smaller than the chain's persistence length as that of a charged rod with the distance between charges $b = 0.17$ nm (there are about 10 base pairs per DNA double helix turn with length 3.4 nm) and by assuming that the effective chain's ionization degree $\alpha \approx 0.15-0.17$ (see, for details, ref 58) we can estimate $\tilde{f}_{K^*}$

$$f_{K^*} \approx \left(\frac{u\alpha^2}{2\kappa b}\right)^2 \frac{k_B T}{l_p^0} \approx \frac{6.92 \times 10^{-4}}{I} pN \tag{64}$$

where I is the solution ionic strength, and $l_p^0 = bK \approx 40$ nm is the bare DNA persistence length. Note that in writing eq 64 we have neglected the logarithmic dependence of the electrostatic tension on the Debye screening length, $\tilde{f}_e \approx -u\alpha^2 \ln(\kappa b)$.

If the opposite inequality holds, $\tilde{f} \geq \tilde{f}_{K^*}$, the effective chain's bending constant decreases with increasing the value of the applied force

$$K_{eff} \approx K\left(\frac{x+y}{xy}\right)^2 \approx K\left(1 + \frac{\tilde{f}_e}{\tilde{f}}\right) \tag{65}$$

Thus, in the large force limit, $\tilde{f} \gg \tilde{f}_e$, the value of the effective chain's bending constant approaches K value. For the DNA molecule the value of electrostatic tension force is on the order of $f_e \approx u\alpha^2 k_B T/b \approx 2.26$ pN.

The lines in Figure 11 correspond to effective chain's bending constant K_{eff} evaluated by using numerically calculated values of the average projection of the unit bond vector on the z-axis $\langle n_z\rangle$. In the large force limit this average value is approximated as $\langle n_z\rangle \approx \tilde{f}/\mu$ (see Section 3). The values of the Lagrange multiplier μ for these plots were obtained by numerically solving the following integral equation

$$1 = \frac{2}{\pi}\int_0^\infty \frac{dq}{Kq^2 + V(q) + \mu} + \left(\frac{\tilde{f}}{\mu}\right)^2 \tag{66}$$

For this procedure we used the value of the chain's bending constant K, the electrostatic interaction parameter $A_{el} = 1$, and the average bond length $b = 0.905\sigma$ from simulations. The agreement between the simulation results and numerically calculated values of the effective chain's bending constant K_{eff} is very good. This comparison between simulation and numerical results suggests that we can use eq 66 for the inverse problem to solve for chain's parameters such as K, A_{el}, and b by using as an input dependence of chain deformation $\langle n_z \rangle = \langle R_z \rangle / bN$ on the applied force f. Thus, overcoming complications arising from the force dependent effect of the electrostatic interactions on the chain's bending properties. Our analysis of the simulation data also indicates that extraction of the DNA parameters from experiments requires consideration of the force dependent effective chain bending constant to account for the scale dependent effect of the electrostatic interactions on the chain's bending rigidity (see discussion above). In their analysis of the DNA stretching data, Baumann et al.[52] fitted the force-elongation curve to the Marko and Siggia[42] expression (see eq 37) with force independent value of the chain bending constant. This fitting procedure provides an average value of the chain's bending constant over the interval of the applied forces. We have attempted to reanalyze the data sets by Baumann et al[52] implementing procedure similar to the one used for extracting effective chain's bending constant from our simulation data (see Figure 11). Unfortunately, the accuracy of the data digitizing procedure from the plots given in ref 52 and the quality of the data sets did not allow us to obtain significant variations of the effective chain's bending constant with the applied force. Thus, more accurate measurements are necessary to prove the force dependence of the chain bending constant experimentally. We hope that our work will inspire a new DNA stretching experiments that will provide more accurate measurements of the chain deformation.

To the end of this section we want to point out that our expression eq 66 has a wider applicability range and uses discrete nature of the charge distribution along the polymer backbone (see eq 15 for definition of the electrostatic interaction term $V(q)$) in comparison with the expression derived by Marko and Siggia.[42]

7. Conclusions

We have used combination of the molecular dynamics simulations and theoretical calculations to study the deformation of a semiflexible polyelectrolyte chain. Our analysis shows that the bond−bond correlation function of a semiflexible polyelectrolyte chain under tension can be approximated by a sum of a constant and two exponential functions. The constant term is due to preferential chain orientation along the direction of the applied force. The sum of the two exponential functions describes the correlations in fluctuations of the bond vectors about the average chain orientation imposed by the applied force. The form of the bond−bond correlation function is a result of the scale dependent contribution of the electrostatic interactions to the chain's elastic and bending modulus. The two different correlation lengths characterizing the decays of the orientational memory between bond vectors describe short-range and long-range orientational correlations. The short-length scale correlation length describes the chain's orientational memory at the distances along the polymer backbone smaller or on the order of the Debye screening length while the long-scale correlation length is responsible for the chains bending properties at the distances larger than the Debye screening length. In the small force limit both correlation lengths are constant. The applied external force first begins to influence the long-scale orientational correlations. This occurs at the value of the reduced force on the order of $\tilde{f} \propto 1/K^*$ (see eq 57 for definition of K^*). For the DNA molecule this crossover takes place at $f \approx 0.1pN$ for typical salt concentration range. In the interval of the applied forces $\tilde{f} > 1/K^*$ at the long-length scales a semiflexible polyelectrolyte chain behaves similar to a neutral chain under tension with the effective chain's bending constant being equal to K^* and with the corresponding long-range correlation length $\lambda_1 \propto (K^*/\tilde{f})^{1/2}$. Thus, the bond orientational correlations decay faster with increasing the value of the applied external force. At the same time the short-length scale correlation length stays unchanged and is still determined by the local electrostatic induced tension, $\lambda_2 \propto (K/\tilde{f}_e)^{1/2}$. The chain deformations start to influence the local chain's deformation modes when the external force becomes on the order of the electrostatic tension force $\tilde{f} \approx \tilde{f}_e$. For the DNA molecule the value of the electrostatic tension force is on the order of $f_e \approx 2.2pN$. In the larger force interval $\tilde{f} > \tilde{f}_e$ the correlation length λ_2 shows behavior similar to that of a neutral chain with the bending constant K under tension $\tilde{f}$, $\lambda_2 \approx (K/\tilde{f})^{1/2}$. Note that in this large force limit the behavior of a semiflexible polyelectrolyte chain becomes independent of the strength of the electrostatic interactions.

The chain's bond−bond correlation properties manifest themselves in the force dependence of a chain size. There are three different chain's deformation regimes depending on the magnitude of the external force f. In the case of weak external forces, $fb/k_BT < 1/K^*$, the mean-square average values of the chain end-to-end distance is a quadratic function of the force magnitude

$$\langle R^2(f) \rangle \approx 2b^2K^*N + (b\tilde{f}K^*N)^2 \tag{67}$$

Note that, in writing eq 67, we have neglected the effect of the electrostatic interactions between remote along the polymer backbone charged pairs that for sufficiently long chains can lead to additional chain swelling.[57] These electrostatic interactions change corresponding exponents for the chain size dependence on the degree of polymerization N and magnitude of the applied force f to those of a chain with effective electrostatic second virial coefficient. The chain swelling effects can be taken into account by using the Pincus blob model[59] or in the framework of the variational approach developed by Morrison et al[60] for deformation of a chain with the excluded volume interactions. It is also important to point out, that for the accessible force interval the swelling effects are more pronounced for flexible polyelectrolyte chains such as single stranded DNA[61] and will be discussed in separate publication.

The behavior of a chain qualitatively changes when $\tilde{f} > 1/K^*$. In this range of parameters the mean-square average value of the chain's end-to-end distance is

$$\langle R^2(f) \rangle \approx \langle R_z \rangle^2 \approx b^2N^2 \left(1 - \frac{1}{\sqrt{\tilde{f}K_{eff}}} \right) \tag{68}$$

This is in line with the results obtained for deformation of a semiflexible chain with force dependent effective chain bending rigidity K_{eff}. It is constant $K_{\text{eff}} \approx K^*$ in the interval of the applied forces $1/K^* < \tilde{f} \leq \tilde{f}_{K^*}$ and is inversely proportional to the magnitude of the applied force $K_{\text{eff}} \approx K(1 + f_e/f)$ for $\tilde{f} \gg \tilde{f}_{K^*}$ (see eq 63 for the definition of $\tilde{f}_{K^*}$). As one can see in the limit of large forces, the value of the effective chain bending constant K_{eff} approaches K value. In this regime the behavior of a polyelectrolyte chain under tension is similar to deformation of a neutral semiflexible chain with the bending constant K

$$\langle R^2(f) \rangle \approx b^2N^2 \left(1 - \frac{1}{\sqrt{K\tilde{f}}} \right) \tag{69}$$

Thus, in this deformation regime the chain size is independent of the salt concentration (see Figures 2).

The developed here model of deformation of semiflexible polyelectrolyte chain can be used to describe elasticity of biological gels made of semiflexible polyelectrolytes.[62−65] The discovered force dependence of the effective chain bending constant could lead to a new nonlinear regime in gel deformation. Another area of research that could benefit from our results is confinement of the semiflexible polyelectrolyte chains inside pores and channels.[27,66−71] In these systems one should expect a decrease of the effective chain's bending constant with decreasing the size of the confining pore. This is because both the external force and the confining pore restrict lateral chain's fluctuations. We will address these problems in future publications.

Acknowledgment. This work was supported by the donors of the Petroleum Research Fund, administered by the American Chemical Society, under Grant PRF#44861-AC7.

Appendix A

In this appendix, we will present analysis of the finite N corrections to the expression of the average projection of the unit bond vector on the z-axis, $\langle n_z\rangle$. In the normal mode representation the chain's potential energy is equal to

$$\frac{U(\{\vec{a}_k\},\vec{f},\mu)}{k_BT} = N\sum_{k=-(N-1)}^{N-1}\left(G(k,\mu)\frac{(\vec{a}_k\cdot\vec{a}_{-k})}{2} - \tilde{f}a_k^z t_k\right) - \frac{N\mu}{2} \tag{A1}$$

where we defined functions

$$G(k,\mu) = K(k\pi/N)^2 + V(k\pi/N) + \mu \tag{A2}$$

and

$$t_k = \frac{1}{N}\sum_{s=0}^{N-1}\exp\left(i\frac{\pi k s}{N}\right) \tag{A3}$$

Note that in the limit of large $N\to\infty$ functions t_k reduce to $\delta_{k,0}$ and one recovers eq 20. Let us evaluate averages over mode amplitudes in two limiting cases of small and large values of the applied force. In the small force limit, $\tilde{f}\ll 1$, we can consider the force term in the rhs of eq A1 as perturbation. In this approximation the average value of the projection of the unit bond vector on the direction of the force is equal to

$$\langle n_z\rangle = \left\langle N^{-1}\sum_{s=0}^{N-1} n_s^z\right\rangle = \sum_{k=-(N-1)}^{N-1}\langle a_k^z\rangle t_k \approx N\tilde{f}\sum_{k=-(N-1)}^{N-1}\langle(a_k^z a_{-k}^z)\rangle_0 t_k t_{-k} \tag{A4}$$

where brackets $\langle\rangle$ and $\langle\rangle_0$ denote averages with the statistical weights corresponding to partition functions $Z(f)$ and $Z(0)$ respectively (see eq 12). In order to calculate the averages in eq A4, we will set $\vec{a}_k = \vec{a}_{-k}$ and use the following relations

$$\langle(a_0^z)^2\rangle_0 = \frac{\langle\vec{a}_0{}^2\rangle_0}{3} = \frac{2}{3\mu N} \tag{A5}$$

$$\langle(a_k^z)^2\rangle_0 = \frac{\langle\vec{a}_k{}^2\rangle_0}{3} = \frac{G(k,\mu)^{-1}}{3N}$$

Note that each vector $\vec{a}_k$ has only two independent components because transformation eq 13 is a linear transformation. Taking eqs A5 into account the r.h.s of eq A4 reduces to

$$\langle n_z\rangle \approx \frac{2\tilde{f}}{3\pi N}\sum_{s,s'=0}^{N-1}\int_0^\infty \frac{\mathrm{d}q\cos(q|s-s'|)}{Kq^2+V(q)+\mu} = \frac{\tilde{f}\langle R_0^2(\mu,K)\rangle}{3N}, \quad \text{for } \tilde{f}\ll 1 \tag{A6}$$

where we defined

$$\langle R_0{}^2(\mu,K)\rangle = \frac{2}{\pi}\sum_{s,s'=0}^{N-1}\int_0^\infty \frac{\mathrm{d}q\cos(q|s-s'|)}{Kq^2+V(q)+\mu} \tag{A7}$$

In obtaining eq A6, we have introduced $q = k\pi/N$, substituted summation by integration and extended the upper integration limit to infinity.

In the case of the large force amplitudes we can assume that the average component of the vectors $\vec{a}_k$ points in the direction of the applied force. Thus, the addition of the external constant force changes the average value of the amplitude of the mode component along z-axes to

$$\langle a_k^z\rangle \approx \tilde{f}t_{-k}/(Kq^2+V(q)+\mu), \quad \text{for } \tilde{f}\gg 1 \tag{A8}$$

resulting in the following expression for the average value of the unit bond vector

$$\langle n_z\rangle \approx \sum_{k=-(N-1)}^{N-1}\langle a_k^z\rangle t_k \approx \frac{2\tilde{f}}{N\pi}\sum_{s,s''=0}^{N-1}\int_0^\infty\frac{\mathrm{d}q\cos((s-s')q)}{Kq^2+V(q)+\mu} - \frac{\tilde{f}}{\mu} = \frac{\tilde{f}\langle R_0^2(\mu,K)\rangle}{N} - \frac{\tilde{f}}{\mu} \tag{A9}$$

Combining eqs A6 and A9 together we have

$$\langle n_z\rangle = \tilde{f}\begin{cases}\langle R_0^2(\mu,K)\rangle/3N, & \tilde{f}\ll 1\\ \langle R_0^2(\mu,K)\rangle/N - 1/\mu, & \tilde{f}\gg 1\end{cases} \tag{A10}$$

where the Lagrange multiplier μ is the solution of the following nonlinear equation see eq 24

$$1 = \frac{2}{\pi}\int_0^\infty\frac{\mathrm{d}q}{Kq^2+V(q)+\mu} + \langle n_z\rangle^2 \tag{A11}$$

To analyze different regimes in eq A10, it is convenient to consider first the case of the neutral chains with $V(q) = 0$. Taking this into account and performing integration and summations in eq A7 one has

$$\langle R_0{}^2(\mu,K)\rangle \approx 2\sqrt{\frac{K}{\mu^3}}\left(N\sqrt{\frac{\mu}{K}} - 1 + \exp\left(-\sqrt{\frac{\mu}{K}}N\right)\right) \tag{A12}$$

The exponential term in the rhs of eq A12 can be neglected when the ratio $N(\mu/K)^{1/2} > 1$, resulting in $\langle R_0{}^2(\mu,K)\rangle \approx 2N/\mu$. Solving eq A11 for μ at the zero force limit, $\langle n_z\rangle = 0$, we obtain for the value of the Lagrange multiplier $\mu(0) = K^{-1}$. Thus, the condition $N(\mu/K)^{1/2} > 1$ transforms to $N/K > 1$. In the large force limit, $\tilde{f}K \gg 1$ (see section 3 for details), $\langle n_z\rangle \approx 1$ and the value of the Lagrange multiplier is equal to $\mu \approx \tilde{f}$. Using this expression for μ one can rewrite the condition as $N(\tilde{f}/K)^{1/2} > 1$. Thus, we can use a zero mode approximation for sufficiently long chains with

$N/K > 1$ or in the interval of sufficiently strong forces such that $\tilde{f} > K/N^2$. Note that the approximation $\langle R_0^2(\mu,K)\rangle \approx 2N/\mu$ provide a qualitatively correct results even in the case $N(\mu/K)^{1/2} \propto 1$.

In the case of the charged systems in the limit of the small q, which dominate contribution to the integral in the rhs of eq A7 for small and intermediate force range, the function

$$Kq^2 + V(q) + \mu \approx \left(K + \frac{u\alpha^2}{4(\kappa b)^2}\right)q^2 + \mu \approx \lambda_1 q^2 + \mu \quad \text{(A13)}$$

The extension of the analysis presented above to the charged systems is straightforward by substituting the bare chain bending constant K by λ_1.

Appendix B

In this appendix, we consider a more general approach to chain deformation when the external force can induce an additional bond stretching such that the equilibrium bond size changes with the force magnitude. The free energy of the system with deformable bonds in the large force limit is

$$\frac{F(b,f,\mu)}{k_B T} \approx N\frac{U_{bond}(b)}{k_B T} + \frac{E_{rod}(b,\kappa)}{k_B T} + \sum_{k=0}^{N-1} \ln\left(K\left(\frac{k\pi}{N}\right)^2 + V\left(\frac{k\pi}{N}\right) + \mu\right) - \frac{N}{2\mu}\left(\frac{fb}{k_B T}\right)^2 - \frac{\mu N}{2} \quad \text{(B1)}$$

where the first term describes the bond energy with a bond length b

$$\frac{U_{bond}(b)}{k_B T} = -\frac{k_{spring} R_{max}^2}{2k_B T}\ln\left(1 - \frac{b^2}{R_{max}^2}\right) + \frac{4\varepsilon_{LJ}}{k_B T}\left(\left(\frac{\sigma}{b}\right)^{12} - \left(\frac{\sigma}{b}\right)^{6}\right) + \frac{\varepsilon_{LJ}}{k_B T} \quad \text{(B2)}$$

The functional form of this interaction potential corresponds to the one used in our simulations. The remaining terms in eq B1 are obtained by evaluating the chain's partition function eq 12 with a logarithmic term accounting for the orientational fluctuations of the bond vectors. Note that in writing eq B1 we have neglected terms that do not depend on the bond length b or the Lagrange multiplier μ. The optimal values of the parameters b and μ are obtained by differentiating the free energy (eq B1) with respect to μ and b. The optimization of the free energy eq B1 with respect to the Lagrange multiplier μ recovers eq 24 in the large force limit

$$1 = \frac{2}{\pi}\int_0^\infty \frac{dq}{Kq^2 + V(q) + \mu} + \left(\frac{fb}{k_B T\mu}\right)^2 \quad \text{(B3)}$$

and optimization with respect to the bond length b results in

$$\frac{U'_{bond}(b)}{k_B T} + \frac{E'_{rod}(b,\kappa)}{k_B TN} + \frac{1}{\pi}\int_0^\infty \frac{V'(q)\,dq}{(Kq^2 + V(q) + \mu)} - \frac{b}{\mu}\left(\frac{f}{k_B T}\right)^2 = 0 \quad \text{(B4)}$$

where $g'(b)$ denotes derivative of a function $g(b)$ with respect to the bond length b.

The analytical solutions of eqs B3 and B4 can be obtained if one approximates the bond potential by a parabolic potential in the following form

$$\frac{U_{bond}(b)}{k_B T} \approx \frac{K_{bond}}{2\sigma^2}(b - b_0)^2 \quad \text{(B5)}$$

where b_0 is the equilibrium bond length without applied force, and K_{bond}/σ^2 is the effective bond elastic constant in terms of the thermal energy $k_B T$. In the case of the neutral chain, eqs B3 and B4 are reduced to

$$1 = \frac{1}{\sqrt{\mu K}} + \left(\frac{fb}{k_B T\mu}\right)^2 \quad \text{(B6)}$$

and

$$\frac{K_{bond}}{\sigma^2}(b - b_0) - \frac{b}{\mu}\left(\frac{f}{k_B T}\right)^2 = 0 \quad \text{(B7)}$$

Since the bond deformation occurs only in the interval of the applied forces for which $fbK/k_B T \gg 1$. The eq B7 can be simplified as follows

$$b \approx b_0 + \frac{f\sigma^2}{K_{bond} k_B T} \quad \text{(B.8)}$$

Appendix C

In this appendix, we will present the calculation details of evaluation of the integrals in eq 43 and present numerical solutions for the variational parameters. We begin with calculation of the second integral in eq 43 to obtain a self-consistent equation coupling the variational parameters μ, A and δ with the system parameters:

$$\frac{2}{\pi}\int_0^\infty \frac{(V(q) - V_{tr}(q))\,dq}{[\tilde{G}^{-1}(q)]^2} = 0 \quad \text{(C1)}$$

where

$$V(q) = 2u\alpha^2 \sum_{m=1}^{N}\left(1 - \frac{m}{N}\right)\frac{\exp(-\kappa bm)}{m^3}(1 + \kappa bm)\left(\sum_{s=1}^{m}(m-s)(1 - \cos(qs))\right) \quad \text{(C2)}$$

$$V_{tr}(q) = \frac{Aq^2}{\delta^2 + q^2} \quad \text{(C3)}$$

and

$$\tilde{G}(q) = \frac{1}{K(z_2^2 - z_1^2)}\left[\frac{\delta^2 - z_1^2}{q^2 + z_1^2} + \frac{z_2^2 - \delta^2}{q^2 + z_2^2}\right] \quad \text{(C4)}$$

The integration in eq C1 can be performed analytically resulting in

$$0 = \frac{1}{K^2(z_2^2 - z_1^2)^2}\left[\left((\delta^2 - z_1^2)^2 I_1(z_1) - \frac{A}{2}\frac{(\delta - z_1)^2}{z_1}\right) + (z_2^2 - \delta^2)^2 I_1(z_2) + (\delta^2 - z_1^2)(z_2^2 - \delta^2) I_2(z_1, z_2) - \frac{A}{2}\left(\frac{(z_2 - \delta)^2}{z_2} + 4\frac{(\delta - z_1)(z_2 - \delta)}{z_1 + z_2}\right)\right] \quad \text{(C5)}$$

where we defined

$$I_1(z) = 2u\alpha^2 \sum_{m=1}^{N} T(m) \sum_{s=1}^{m} (m-s) g_1(s,z) \tag{C6}$$

$$I_2(z_1,z_2) = 2u\alpha^2 \sum_{m=1}^{N} T(m) \sum_{s=1}^{m} (m-s) g_2(s,z_1,z_2) \tag{C7}$$

$$T(m) = \left(1-\frac{m}{N}\right)\frac{\exp(-\kappa bm)}{m^3}(1+\kappa bm) \tag{C8}$$

$$g_1(s,z) = \frac{2}{\pi}\int_0^\infty \frac{(1-\cos(qs))}{(q^2+z^2)^2}\,dq = \frac{1}{2z^3}(1-(1+sz)\exp(-sz)) \tag{C9}$$

$$g_2(s,z_1,z_2) = \frac{4}{\pi}\int_0^\infty \frac{(1-\cos(qs))}{(q^2+z_1^2)(q^2+z_2^2)}\,dq = \frac{2}{(z_2^2-z_1^2)}\left(\frac{1-\exp(-sz_1)}{z_1}-\frac{1-\exp(-sz_2)}{z_2}\right) \tag{C10}$$

It is useful to introduce a new reduced variables such that

$$x = \frac{z_2}{\delta} \quad \text{and} \quad y = \frac{z_1}{\delta} \tag{C11}$$

where we assumed that $x > 1$, and $y < 1$. Solving for the parameter δ, we have

$$z_1^2 z_2^2 = \frac{\delta^2\mu}{K} \Rightarrow \delta = \frac{1}{xy}\sqrt{\frac{\mu}{K}} \tag{C12}$$

This leads to the following expressions for the smallest and largest roots

$$z_1 = \frac{1}{x}\sqrt{\frac{\mu}{K}}; \quad z_2 = \frac{1}{y}\sqrt{\frac{\mu}{K}} \tag{C13}$$

Using this representation we can also obtain value of the parameter A:

$$z_1^2 + z_2^2 = \delta^2 + \frac{\mu}{K} + \frac{A}{K} \Rightarrow \frac{A}{\delta^2} = K(x^2-1)(1-y^2) \tag{C14}$$

In these new variables, we can rewrite eq C5 as combination of two equations

$$f_1(x,y,\mu) = \left(z_1 I_1(z_1) - K\frac{(x^2-1)(1-y)}{2\quad(1+y)}\right) = 0$$

$$f_2(x,y,\mu) = \left[\frac{(x^2-1)}{(1-y^2)} z_2^2 I_1(z_2) + z_2^2 I_2(z_1,z_2) - \frac{(\mu K)^{1/2}x}{2y}\left(\frac{(x-1)^2}{x} + 4\frac{(1-y)(x-1)}{x+y}\right)\right] = 0 \tag{C15}$$

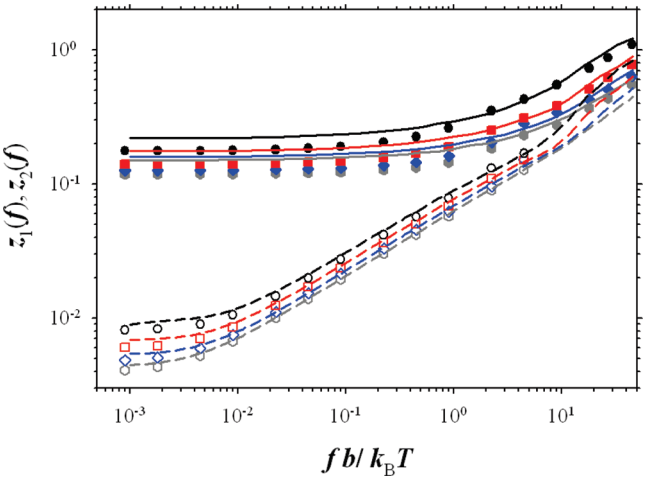

Figure 12. Dependence of the parameters $z_1(f)$ (open symbols and dashed lines) and $z_2(f)$ (filled symbols and solid lines) on the value of the reduced applied force fb/k_BT obtained from the function $G(l)$ (symbols) and from the variational principle (lines) for semiflexible polyelectrolyte chains with the degree of polymerization $N_m = 200$, electrostatic coupling constant $A_{el} = 1.0$, Debye screening length $\kappa^{-1} = 20\sigma$ and for different values of the bending constant: $K = 40.0$ (black circles), $K = 80.0$ (red squares), $K = 120.0$ (blue rhombs), and $K = 160.0$ (gray hexagons).

The eqs C15 have to be supplemented by a normalization condition eq 48

$$f_3(x,y,\mu) = 1 - \frac{1+xy}{(x+y)\sqrt{K\mu}} - \langle n_z\rangle^2 = 0 \tag{C16}$$

where we can use the following crossover expression for the average value of the projection of the unit bond vector

$$\langle n_z\rangle = \frac{\tilde{f}}{\mu}\left(1 - \frac{1}{3}\frac{\mu(0)}{(\mu(0)+\tilde{f})}\right) \tag{C17}$$

where $\mu(0)$ is the value of the Lagrange multiplier at zero applied force. The optimal values of the parameters K^*, μ, and δ can be found by minimizing a function

$$\chi(x,y,\mu) = f_1^2(x,y,\mu) + f_2^2(x,y,\mu) + f_3^2(x,y,\mu) \tag{C18}$$

Figure 12 shows comparison between the roots z_1 and z_2 obtained from the numerically calculated correlation functions eq 23 and ones calculated from the variational approach by minimizing a χ-function eq C18. The agreement between the values of the bending rigidities is reasonably good. The agreement between variational principle and direct integration results improves with increasing the initial chain's bending rigidity K and magnitude of the applied force.

References and Notes

(1) Alessandrini, A.; Facci, P. AFM: a versatile tool in biophysics. *Meas. Sci. Technol.* **2005**, *16* (6), R65–R92.
(2) Bustamante, C.; Smith, S. B.; Liphardt, J.; Smith, D. Single-molecule studies of DNA mechanics. *Curr. Opin. Struct. Biol.* **2000**, *10* (3), 279–285.
(3) Smith, S. B.; Cui, Y. J.; Bustamante, C. Overstretching B-DNA: The elastic response of individual double-stranded and single-stranded DNA molecules. *Science* **1996**, *271* (5250), 795–799.
(4) Chen, G.; Wen, J. D.; Tinoco, I. Single-molecule mechanical unfolding and folding of a pseudoknot in human telomerase RNA. *RNA-a Publ. RNA Soc.* **2007**, *13*, 2175–2188.

(5) Dame, R. T. Single-molecule micromanipulation studies of DNA and architectural proteins. *Biochem. Soc. Trans.* **2008**, *36*, 732–737.
(6) Deniz, A. A.; Mukhopadhyay, S.; Lemke, E. A. Single-molecule biophysics: at the interface of biology, physics and chemistry. *J. R. Soc. Interface* **2008**, *5* (18), 15–45.
(7) Fuller, D. N.; Raymer, D. M.; Kottadiel, V. I.; Rao, V. B.; Smith, D. E. Single phage T4 DNA packaging motors exhibit large force generation, high velocity, and dynamic variability. *Proc. Natl. Acad. Sci. U.S.A.* **2007**, *104*, 16868–16873.
(8) Greenleaf, W. J.; Woodside, M. T.; Block, S. M. High-resolution, single-molecule measurements of biomolecular motion. *Annu. Rev. Biophys. Biomol. Struct.* **2007**, *36*, 171–190.
(9) Hanke, A.; Ochoa, M. G.; Metzler, R. Denaturation transition of stretched DNA. *Phys. Rev. Lett.* **2008**, *100* (1), 018106-1–018106-4.
(10) Kada, G.; Kienberger, F.; Hinterdorfer, P. Atomic force microscopy in bionanotechnology. *Nano Today* **2008**, *3* (1−2), 12–19.
(11) Lankas, F.; Sponer, J.; Hobza, P.; Langowski, J. Sequence-dependent elastic properties of DNA. *J. Mol. Biol.* **2000**, *299*, 695–709.
(12) Lionnet, T.; Dawid, A.; Bigot, S.; Barre, F. X.; Saleh, O. A.; Heslot, F.; Allemand, J. F.; Bensimon, D.; Croquette, V. DNA mechanics as a tool to probe helicase and translocase activity. *Nucleic Acids Res.* **2006**, *34*, 4232–4244.
(13) Marko, J. F. Micromechanical studies of mitotic chromosomes. *Chromosome Res.* **2008**, *16*, 469–497.
(14) Morozov, A. V.; Fortney, K.; Gaykalova, D. A.; Studitsky, V. M.; Widom, J.; Siggia, E. D. Using DNA mechanics to predict in vitro nucleosome positions and formation energies. *Nucleic Acids Res.* **2009**, *37*, 4707–4722.
(15) Neuman, K. C.; Nagy, A. Single-molecule force spectroscopy: optical tweezers, magnetic tweezers and atomic force microscopy. *Nat. Meth.* **2008**, *5* (6), 491–505.
(16) Prevost, C.; Takahashi, M.; Lavery, R. Deforming DNA: From Physics to Biology. *ChemPhysChem* **2009**, *10*, 1399–1404.
(17) Ritort, F. Single-molecule experiments in biological physics: methods and applications. *J. Phys.: Condens. Matter* **2006**, *18*, R531–R583.
(18) Rouzina, I.; Bloomfield, V. A. Force-induced melting of the DNA double helix - 1. Thermodynamic analysis. *Biophys. J.* **2001**, *80*, 882–893.
(19) Seidel, R.; Dekker, C. Single-molecule studies of nucleic acid motors. *Curr. Opin. Struct. Biol.* **2007**, *17* (1), 80–86.
(20) Shokri, L.; McCauley, M. J.; Rouzina, I.; Williams, M. C. DNA overstretching in the presence of glyoxal: Structural evidence of force-induced DNA melting. *Biophys. J.* **2008**, *95*, 1248–1255.
(21) Sischka, A.; Toensing, K.; Eckel, R.; Wilking, S. D.; Sewald, N.; Ros, R.; Anselmetti, D. Molecular mechanisms and kinetics between DNA and DNA binding ligands. *Biophys. J.* **2005**, *88*, 404–411.
(22) Tinoco, I. Force as a useful variable in reactions: Unfolding RNA. *Annu. Rev. Biophys. Biomol. Struct.* **2004**, *33*, 363–385.
(23) Williams, M. C.; Rouzina, I. Force spectroscopy of single DNA and RNA molecules. *Current Opinion in Structural Biology* **2002**, *12*, 330–336.
(24) Zhang, H. Y.; Marko, J. F. Maxwell relations for single-DNA experiments: Monitoring protein binding and double-helix torque with force-extension measurements. *Phys. Rev. E* **2008**, *77*, 031916.
(25) Kim, J. H.; Shi, W. X.; Larson, R. G. Methods of stretching DNA molecules using flow fields. *Langmuir* **2007**, *23*, 755–764.
(26) Hu, X.; Wang, S. N.; Lee, L. J. Single-molecule DNA dynamics in tapered contraction-expansion microchannels under electrophoresis. *Phys. Rev. E* **2009**, *79*, 041911.
(27) Hsieh, S. S.; Liou, J. H. DNA molecule dynamics in converging-diverging microchannels. *Biotechnol. Appl. Biochem.* **2009**, *52* (1), 29–40.
(28) Ladoux, B.; Doyle, P. S. Stretching tethered DNA chains in shear flow. *Europhys. Lett.* **2000**, *52*, 511–517.
(29) Larson, J. W.; Yantz, G. R.; Zhong, Q.; Charnas, R.; D'Antoni, C. M.; Gallo, M. V.; Gillis, K. A.; Neely, L. A.; Phillips, K. M.; Wong, G. G.; Gullans, S. R.; Gilmanshin, R. Single DNA molecule stretching in sudden mixed shear and elongational microflows. *Lab Chip* **2006**, *6*, 1187–1199.
(30) Larson, R. G. The rheology of dilute solutions of flexible polymers: Progress and problems. *J. Rheol.* **2005**, *49* (1), 1–70.
(31) Haber, C.; Wirtz, D. Magnetic tweezers for DNA micromanipulation. *Rev. Sci. Instrum.* **2000**, *71*, 4561–4570.
(32) Gosse, C.; Croquette, V. Magnetic tweezers: Micromanipulation and force measurement at the molecular level. *Biophys. J.* **2002**, *82*, 3314–3329.
(33) Hormeno, S.; Arias-Gonzalez, J. R. Exploring mechanochemical processes in the cell with optical tweezers. *Biol. Cell* **2006**, *98*, 679–695.
(34) McCauley, M. J.; Williams, M. C. Review: Optical tweezers experiments resolve distinct modes of DNA-protein binding. *Biopolymers* **2009**, *91* (4), 265–282.
(35) Mangeol, P.; Cote, D.; Bizebard, T.; Legrand, O.; Bockelmann, U. Probing DNA and RNA single molecules with a double optical tweezer. *Eur. Phys. J. E* **2006**, *19*, 311–317.
(36) Dong, M. D.; Hovgaard, M. B.; Mamdouh, W.; Xu, S. L.; Otzen, D. E.; Besenbacher, F. AFM-based force spectroscopy measurements of mature amyloid fibrils of the peptide glucagon. *Nanotechnology* **2008**, *19*, 384013.
(37) Fisher, T. E.; Marszalek, P. E.; Fernandez, J. M. Stretching single molecules into novel conformations using the atomic force microscope. *Nat. Struct. Biol.* **2000**, *7* (9), 719–724.
(38) Hansma, H. G.; Kasuya, K.; Oroudjev, E. Atomic force microscopy imaging and pulling of nucleic acids. *Curr. Opin. Struct. Biol.* **2004**, *14*, 380–385.
(39) Hugel, T.; Grosholz, M.; Clausen-Schaumann, H.; Pfau, A.; Gaub, H.; Seitz, M. Elasticity of single polyelectrolyte chains and their desorption from solid supports studied by AFM based single molecule force spectroscopy. *Macromolecules* **2001**, *34*, 1039–1047.
(40) Ke, C.; Humeniuk, M.; S-Gracz, H.; Marszalek, P. E. Direct measurements of base stacking interactions in DNA by single-molecule atomic-force spectroscopy. *Phys. Rev. Lett.* **2007**, *99* (1), 018302-1–018302-4.
(41) Dessinges, M. N.; Maier, B.; Zhang, Y.; Peliti, M.; Bensimon, D.; Croquette, V. Stretching single stranded DNA, a model polyelectrolyte. *Phys. Rev. Lett.* **2002**, *89*, 24810211–248102-4.
(42) Marko, J. F.; Siggia, E. D. Stretching DNA. *Macromolecules* **1995**, *28*, 8759–8770.
(43) Skolnick, J.; Fixman, M. Electrostatic persistence length of a wormlike polyelectrolyte. *Macromolecules* **1977**, *10*, 944–948.
(44) Odijk, T. Polyelectrolytes near the rod limit. *J. Polym. Sci. Polym. Phys. Ed.* **1977**, *15*, 477–483.
(45) Barrat, J. L.; Joanny, J. F. Persistence length of polyelectrolyte chains. *Europhys. Lett.* **1993**, *25*, 333–338.
(46) Ha, B. Y.; Thirumalai, D. Persistence length of flexible polyelectrolyte chains. *J. Chem. Phys.* **1999**, *110*, 7533–7541.
(47) Netz, R. R.; Orland, H. Variational theory for a single polyelectrolyte chain. *Eur. Phys. J. B* **1999**, *8*, 81–98.
(48) Podgornik, R.; Hansen, P. L.; Parsegian, V. A. Elastic moduli renormalization in self-interacting stretchable polyelectrolytes. *J. Chem. Phys.* **2000**, *113*, 9343–9350.
(49) Dobrynin, A. V. Theory and simulations of charged polymers: From solution properties to polymeric nanomaterials. *Curr. Opin. Colloid Interface Sci.* **2008**, *13*, 376–388.
(50) Dobrynin, A. V.; Rubinstein, M. Theory of polyelectrolytes in solutions and at surfaces. *Prog. Polym. Sci.* **2005**, *30*, 1049–1118.
(51) Ullner, M. Comments on the scaling behavior of flexible polyelectrolytes within the Debye-Huckel approximation. *J. Phys. Chem. B* **2003**, *107*, 8097–8110.
(52) Baumann, C. G.; Smith, S. B.; Bloomfield, V. A.; Bustamante, C. Ionic effects on the elasticity of single DNA molecules. *Proc. Natl. Acad. Sci. U.S.A.* **1997**, *94*, 6185–6190.
(53) Gubarev, A.; Carrillo, J.-M. Y.; Dobrynin, A. V. Scale dependent electrostatic stiffening in biopolymers. *Macromolecules* **2009**, *42*, 5851–5860.
(54) Bouchiat, C.; Wang, M. D.; Allemand, J. F.; Strick, T.; Block, S. M.; Croquette, V. Estimating the persistence length of a worm-like chain molecule from force-extension measurements. *Biophys. J.* **1999**, *76*, 409–413.
(55) Frenkel, D.; Smit, B., *Understanding Molecular Simulations*; Academic Press: New York, 2002.
(56) Plimpton, S. J. Fast parallel algorithms for short-range molecular dynamics. *J.Comp.Phys.* **1995**, *117*, 1–19 lammps.sandia.gov.
(57) Jackson, J. D. *Classical Electrodynamics*; John Wiley & Sons: New York, 1998.
(58) Dobrynin, A. V.; Carrillo, J.-M. Y. Swelling of biological and semiflexible polyelectrolytes. *J. Phys.—Condens. Matter* **2009**, *21*, 424112.
(59) Rubinstein, M.; Colby, R. H. *Polymer Physics*; Oxford University Press: New York, 2003.
(60) Morrison, G.; Hyeon, C.; Toan, N. M.; Ha, B. Y.; Thirumalai, D. Stretching homopolymers. *Macromolecules* **2007**, *40*, 7343–7353.

(61) Saleh, O. A.; McIntosh, D. B.; Pincus, P.; Ribeck, N. Nonlinear Low-Force Elasticity of Single-Stranded DNA Molecules. *Phys. Rev. Lett.* **2009**, *102*, 068301−1–4.
(62) MacKintosh, F. C., Elasticity and dynamics of cytoskeletal filaments and their networks. In *Soft condensed matter physics in molecular and cell biology*; Poon, W. C. K.; Andelman, D., Eds.; Taylor & Francis: New York, 2006; pp 139−155.
(63) Blundell, J. R.; Terentjev, E. M. Forces and extensions in semiflexible and rigid polymer chains and filaments. *J. Phys. A: Math. Theor.* **2007**, *40*, 10951–10964.
(64) Blundell, J. R.; Terentjev, E. M. Stretching semiflexible filaments and their networks. *Macromolecules* **2009**, *42*, 5388–5394.
(65) Kabla, A.; Mahadevan, L. Nonlinear mechanics of soft fibrous networks. *J. R. Soc. Interface* **2007**, *4* (12), 99–106.
(66) Jun, S.; Thirumalai, D.; Ha, B. Y. Compression and stretching of a self-avoiding chain in cylindrical nanopores. *Phys. Rev. Lett.* **2008**, *101*, 138101-1–138101-4.
(67) Kumemura, M.; Collard, D.; Yamahata, C.; Sakaki, N.; Hashiguchi, G.; Fujita, H. Single DNA molecule isolation and trapping in a microfluidic device. *ChemPhysChem* **2007**, *8*, 1875–1880.
(68) Reisner, W.; Morton, K. J.; Riehn, R.; Wang, Y. M.; Yu, Z. N.; Rosen, M.; Sturm, J. C.; Chou, S. Y.; Frey, E.; Austin, R. H. Statics and dynamics of single DNA molecules confined in nanochannels. *Phys. Rev. Lett.* **2005**, *94*, 196101-1–196101-4.
(69) Reccius, C. H.; Mannion, J. T.; Cross, J. D.; Craighead, H. G. Compression and free expansion of single DNA molecules in nanochannels. *Phys. Rev. Lett.* **2005**, *95*, 268101-1–268101-4.
(70) Strychalski, E. A.; Levy, S. L.; Craighead, H. G. Diffusion of DNA in nanoslits. *Macromolecules* **2008**, *41*, 7716–7721.
(71) Tegenfeldt, J. O.; Prinz, C.; Cao, H.; Chou, S.; Reisner, W. W.; Riehn, R.; Wang, Y. M.; Cox, E. C.; Sturm, J. C.; Silberzan, P.; Austin, R. H. The dynamics of genomic-length DNA molecules in 100-nm channels. *Proc. Natl. Acad. Sci. U.S.A.* **2004**, *101*, 10979–10983.